



National Library of Canada
Collections Development Branch

Canadian Theses on
Microfiche Service

Bibliothèque nationale du Canada
Direction du développement des collections

Service des thèses canadiennes
sur microfiche

NOTICE

The quality of this microfiche is heavily dependent upon the quality of the original thesis submitted for microfilming. Every effort has been made to ensure the highest quality of reproduction possible.

If pages are missing, contact the university which granted the degree.

Some pages may have indistinct print especially if the original pages were typed with a poor typewriter ribbon or if the university sent us a poor photocopy.

Previously copyrighted materials (journal articles, published tests, etc.) are not filmed.

Reproduction in full or in part of this film is governed by the Canadian Copyright Act, R.S.C. 1970, c. C-30. Please read the authorization forms which accompany this thesis.

THIS DISSERTATION
HAS BEEN MICROFILMED
EXACTLY AS RECEIVED

AVIS

La qualité de cette microfiche dépend grandement de la qualité de la thèse soumise au microfilmage. Nous avons tout fait pour assurer une qualité supérieure de reproduction.

S'il manque des pages, veuillez communiquer avec l'université qui a conféré le grade.

La qualité d'impression de certaines pages peut laisser à désirer, surtout si les pages originales ont été dactylographiées à l'aide d'un ruban usé ou si l'université nous a fait parvenir une photocopie de mauvaise qualité.

Les documents qui font déjà l'objet d'un droit d'auteur (articles de revue, examens publiés, etc.) ne sont pas microfilmés.

La reproduction, même partielle, de ce microfilm est soumise à la Loi canadienne sur le droit d'auteur, SRC 1970, c. C-30. Veuillez prendre connaissance des formules d'autorisation qui accompagnent cette thèse.

LA THÈSE A ÉTÉ
MICROFILMÉE TELLE QUE
NOUS L'AVONS REÇUE

TIME DOMAIN MODELLING
OF
DIGITAL PLL FOR A.C.MOTOR SPEED CONTROL

by

Manmohan Mittal

A Thesis
presented to the School of Graduate Studies
and Research, University of Ottawa
in partial fulfillment of the
requirements for the degree of
Master of Applied Sciences (M.A.Sc.)
in
ELECTRICAL ENGINEERING

Ottawa, Ontario, CANADA, 1981



Manmohan Mittal, Ottawa, Canada, 1981

The University of Ottawa requires the signatures of all persons using or photocopying this thesis. Please sign below, and give address and date.

ABSTRACT

A time domain model of an adjustable and precise speed-controlled AC drive system has been developed and simulated on a digital computer. In this analysis, starting transients as well as steady state speed control performance of the system have been studied. In order to improve the starting performance significantly, a modification has been incorporated in the control scheme for the starting period only. This modification avoids traditional oscillatory behavior of the induction motor and reduces undesired high current peaks (with a high starting torque).

To verify the validity of the time domain model and the simulation method used in this analysis, the computed results were compared and found matching favourably with those reported in the literature [1,5]

The model has been simulated in two different ways. In the first case, it needs an inversion of a time dependent matrix in every step of integration which is a most inefficient computational operation. But for efficient computation, a second method has been tried, where the voltage equations for stator and rotor circuits of the motor were developed separately to avoid the inversion of the matrix.

ACKNOWLEDGEMENT

The author expresses his deepest gratitude to his advisor, Professor N.U.Ahmed, for his generous encouragement, understanding and invaluable guidance throughout this work, without which this thesis would have not been possible.

He also wishes to express his sincere thanks to Professor K.F.Schenk for his very helpful suggestions/comments, discussions and encouragement for the early completion of this work.

Special thanks to all the Graduate students and staff members of the Department of Electrical Engineering especially to S.Boy, T.E.Dabbous, S.K.Biswas and Peter Uko for their timely help, encouragement and advices.

Thanks to the Natural Sciences & Engineering Research Council of CANADA and Department of Electrical Engineering for the financial assistance provided throughout the duration of this work.

And last but not the least, the author is highly indebted to his wife Shashi Mittal and his son Vivek for their enormous patience and constant encouragement during this period.

NOMENCLATURE

d	=	Phase/firing angle
D_1	=	Phase Detector Constant
f_v	=	Frequency of optical speed encoder
f_R	=	Frequency of reference oscillator
I_s, I_r	=	Current Vectors
J	=	Moment of inertia of motor & load
K	=	Friction coefficient
K_2	=	VCO constant
K_3	=	Triggering Ckt. Constant
L_{ss}, L_{rr}	=	Self Inductance Matrices
L_{sr}, L_{rs}	=	Mutual Inductance Matrices
L_a	=	Self inductance amplitude
M	=	Mutual inductance amplitude
P	=	No. of Poles
p	=	d/dt
R_1, R_2, C	=	Filter components
R_s, R_r	=	Diagonal Matrix of Resistances
r	=	Rotor parameter subscripts
s	=	Stator parameter subscripts
T_e	=	Internal electrical torque
T_L	=	Load torque
V_s, V_r	=	Voltage Vectors
V_{smax}	=	Max. Amplitude of AC supply

ω = Angular frequency of Inverter output
 ω_c = VCO central frequency
 ω_m = Angular speed of motor
 ω_s = Angular frequency of AC supply

TABLE OF CONTENTS

ABSTRACT	iv
ACKNOWLEDGEMENT	v
NOMENCLATURE	vi
INTRODUCTION	xii
Chapter	page
I. BASIC PRINCIPLE AND SYSTEM DESCRIPTION	1
Basic Principle of a PLL	1
Application of PLLs in Motor Speed Control	3
Modification Proposed	5
II. FUNCTIONAL DESCRIPTION & MATHEMATICAL MODELLING	7
Optical Speed Encoder:	7
Phase-Frequency Detector:	8
Filter:	10
Digital Voltage Controlled Oscillator:	11
Phase Controlled Rectifier & Triggering Circuit	
:	13
Three Phase-controlled Rectifier	13
Triggering Circuits:	19
Voltage Source Inverter & Triggering Circuit :	21
Voltage Source Inverter	21
Triggering and Logic Circuits:	24
Squirrel Cage Induction Motor:	25
Steady State Performance:	27
Adjustable Frequency Operation of Induction	
Motor:	32
Mathematical Model	37
III. DEVELOPMENT OF TIME DOMAIN STATE SPACE MODEL	39
IV. DIGITAL SIMULATION & NUMERICAL RESULTS	45
DIGITAL SIMULATION	45
NUMERICAL RESULTS	62

CONCLUSION	65
APPENDIX - A	68
REFERENCES	92

LIST OF FIGURES

Figure		Page
1.1	Block Diagram of Basic Phase-Locked Loop	2
1.2	Block Diagram - Digital PLL for Motor Speed Control	4
2.1	Digital Optical Speed Encoder	8
2.2	Digital Phase-Frequency Detector and Characteristic	9
2.3	Active Filter	11
2.4	Digital Voltage Controlled Oscillator	12
2.5	Three Phase-Controlled Rectifier	14
2.6	Waveforms for The Phase-Controlled Rectifier	16
2.7	Block Diagram of Triggering Circuit for Controlled Rectifier	20
2.8	Standard Mc Murray Voltage Source Inverter	22
2.9	Waveforms for Voltage Source Inverter	23
2.10	Block Diagram of Triggering & Logic Circuit For VSI	25
2.11	Single Phase Equivalent Circuit of Induction Motor	26
2.12	Torque-Speed Characteristic of Induction Motor	30
2.13	Torque-Speed/Torque-Slip curves with variable frequency supply	34
2.14	Break down and Starting torques Vs Stator Frequency	35
2.15	Torque-Speed Characteristics at different frequencies	36
4.1	Flow Chart For Simulation	46
4.2	Transient Speed Build-up during Starting (without Harmonics)	47
4.3	Transient Current during Starting (without Harmonics)	48
4.4	Transient Torque-Time Characteristics during Starting (without Harmonics)	49
4.5	Transient Torque-Speed Characteristics during Starting (without Harmonics)	50

Figure		Page
4.6	Transient Acceleration-Speed Curves during Starting (without harmonics)	51
4.7	Inverter frequency-time curve during starting	52
4.8	Inverter frequency-speed curve during starting	53
4.9	Computed waveforms of inverter output voltages	54
4.10	Starting Transients with/without control (no harmonics)	55
4.10A	Transient speed build-up curves obtained by two different ways of simulations for efficient computations	56
4.11	Transient speed build-up during starting (with 5th and 7th harmonics)	57
4.12	Transient current during starting (with 5th and 7th harmonics)	58
4.13	Transient torque-time curves during starting (with 5th and 7th harmonics)	59
4.14	Transient torque-speed curves during starting (with 5th and 7th harmonics)	60
4.15	Starting Transients with control having 5th, 7th harmonics	61
4.16	No-load/Full-load response	63

INTRODUCTION

The degree of accuracy and sophistication of speed control required in industrial drives basically depend on the application. In some applications the open loop regulation of the drive motor is adequate. In others feedback control is required for better performance. Conventionally, this is achieved by an analog servo feedback system in which any change in speed is sensed by a tachometer and compared with a fixed reference voltage to generate a correction signal. However, this analog feedback system is not satisfactory in some applications where excellent speed regulation and fast dynamic response is required. These features can be achieved by using a Digital Phase-Locked Loop (PLL) method. In the phase-locked loop method, motor speed is converted to a digital pulse train which is synchronized with the reference digital pulse train. In this way, by locking onto a reference frequency precise control of motor speed is achieved.

Automation of production industries on an increasing scale has resulted in an increase in demand of adjustable and precise speed controlled drive systems such as those used for conveyors, rolling, textile and paper mills etc. In the past DC motors were widely used for this purpose. But

in recent years due to numerous developments in the technology of solid state devices like IC's and thyristors, it has been possible to build inexpensive, compact and reliable Phase-Locked Loops and power supplies of adjustable frequency and voltage. This development has made it possible, to use AC motors (instead of DC motors) for adjustable and precise speed controlled drive systems. AC motors such as squirrel cage induction motors are robust, rugged and economical.

Recently, a few applications of such drive systems using AC/DC motor and PLL have been reported [1,2,3]. In these reports a frequency domain method has been used to model and analyse the ~~steady~~ state performance of the complete drive system. Besides precise speed control, the starting of large AC motors is also of great concern. This is due to the very high initial currents and oscillatory behavior. This has increased interest in the study of transient performance of adjustable speed AC drive system having an induction motor. For efficient performance, it is therefore necessary to study both steady state and transient performance of the system before implementation (which is not possible by frequency domain method).

For this purpose, in this thesis, a time domain model of the complete system (Fig.1.2) has been developed and simulated. The time domain analysis as presented here

provides valuable information on starting transients along with speed control performance. To verify the validity of the model and simulation method, the computed results for speed control performance have been compared with the reported test results [1]. Further, the control scheme has been modified (as shown in Fig.1.2) in order to improve the starting performance with respect to the following characteristics:

- (i) fast & smooth speed pickup
- (ii) low current peaks
- (iii) high torque.

Due to this modification, starting performance was improved significantly.

In the next paragraphs, an overview of the thesis has been presented. In chapter one, the basic principle and application of a PLL in motor speed control including the modification in the control scheme for improving starting performance and operational description of the system have been discussed.

In chapter two, before presenting the mathematical model for each module of the system, a functional description is described for different modules of the complete system. In chapter three, using a mathematical representation for different modules developed in the previous chapter, a state space model has been developed for the complete dynamics of

the system. Later on, it is used for digital simulation in chapter four, where numerical results are also discussed.

Lastly this thesis has been concluded with the scope of further research in this field of interest as perceived by the author.

Chapter I

BASIC PRINCIPLE AND SYSTEM DESCRIPTION

In this chapter, the basic principle of a PLL and its application to the control of motor speed and starting currents (with high torque) have been described. After the introduction of PLLs, the operating principle of the complete drive system and modified control scheme have been explained.

1.1 BASIC PRINCIPLE OF A PLL

A basic PLL consists of a phase detector/comparator, a loop filter, voltage-controlled oscillator (VCO) and reference oscillator. The block diagram of the basic phase-locked loop is depicted in Fig.1.1. The comparator generates a voltage which is proportional to the difference in frequency or phase between a voltage controlled oscillator signal f_v and a reference oscillator signal f_R . This dc error voltage is filtered to produce the required dynamic response and applied to the modulating input of the VCO. The output frequency of the VCO is inversely proportional to its input voltage.

If the VCO output is lower in frequency or lags in phase with that of the reference oscillator, the error voltage

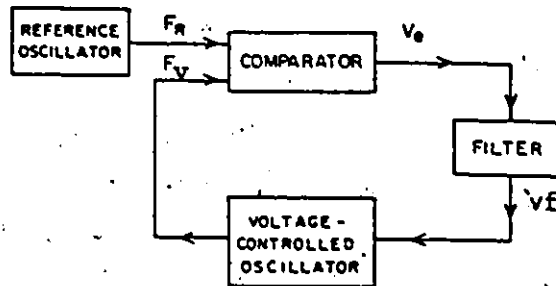


Figure 1.1 - Block Diagram of Basic Phase-Locked Loop (PLL)

appearing at the output of the comparator will decrease. The output frequency of the VCO will then increase (or gain in phase) to compensate for the original error. The error voltage is zero only when the two signals are exactly in phase. A slight lead or lag between the two will result in a corrective voltage and compensation will automatically occur. In this way, with a properly designed filter, the output frequency of the VCO can be made to phase lock with, and therefore track with extreme precision, the frequency of the reference oscillator.

The accuracy with which the VCO output frequency tracks the reference frequency is dependent on the dynamic characteristics of the feed back loop and limited ultimately only by the stability of the reference oscillator.

1.2 APPLICATION OF PLLS IN MOTOR SPEED CONTROL

Phase-Locked Loops were developed in the 1930's and have since been extensively used in communication systems. Although the primary application for PLLs has been in frequency synchronisation of receivers, a lesser known application area has now turned out to be almost equally important - the precise control of the motor speed. By locking onto a reference frequency, speed accuracies of $\pm 0.002\%$ are possible, which represents almost a hundred fold improvement over earlier methods of speed regulation [4]. The conventional method of motor speed control is with analog servos. However, it was not until the past few years, when PLLs could be assembled with IC's, that they became economical enough for such applications and relatively simple to design into systems.

In this thesis, a typical system (as shown in Fig.1.2) for control of induction motor's speed and starting current, has been studied and analysed. The closed loop speed-controlled drive system is comprised of a phase detector, filter, VCO, phase controlled rectifier, voltage source inverter, induction motor and an optical speed encoder. Basically, the system configuration is very similar to basic PLL in which the VCO block has been replaced by a combination of phase-controlled rectifier, voltage source inverter (VSI), induction motor and digital optical-speed encoder. The use of an induction motor and other blocks as

VCO in PLL increases the complexity of the loop design and response time of the overall system.

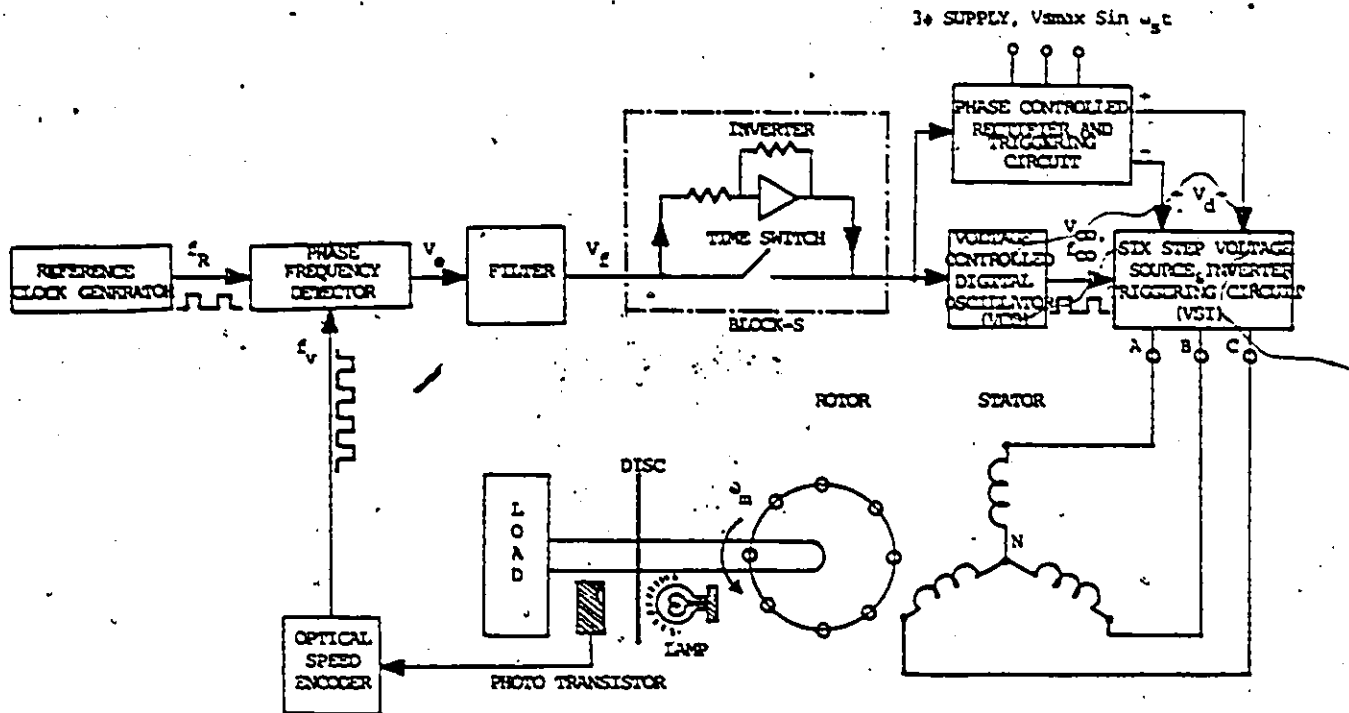


Figure 1.2 - Block Diagram - Digital PLL for Induction Motor Speed Control

The feed back pulse train of frequency f_v (proportional to the actual motor angular speed ω_m) from the optical speed encoder is compared by a digital phase-frequency detector with the reference pulse train of frequency f_R from the crystal clock. The detector output error voltage (V_e) is filtered and amplified. The filtered error voltage V_f is used to modify both the dc output (V_d) of the controlled

rectifier and the frequency (f_{co}) of the VCO. In turn it changes the amplitude as well as frequency of the VSI output. Then the VSI output is fed to the induction motor. As a result, the motor speed changes thereby reducing the frequency difference between the two pulse trains. By locking of the PLL, the induction motor speed is perfectly synchronised with the reference speed.

1.3 MODIFICATION PROPOSED

As mentioned in the introduction, the starting current and oscillatory behavior of the induction motor is also of great concern. The starting performance of the induction motor could be improved significantly, if the input voltage and frequency to the motor are increased smoothly (instead of a step input voltage)[6]. Here, a simple modification in the control scheme (used for speed control only), has been proposed to improve the starting performance of the system substantially. In this modification, to have positive feedback (instead of negative feedback), a inverter block (for changing the sign of V_f) is introduced just after the filter block with a time switch (as shown in Fig.1.2). As a result, the VCO frequency f_{co} and phase controlled rectifier d.c.voltage V_d are now proportional to the filtered error voltage V_f (instead of inversely proportional to the V_f). This is used only during the starting period. The V_d and f_{co} inputs to the VSI increase the amplitude as well as

frequency of the VSI output voltages (input to the motor) linearly with the increase of actual motor speed (as shown in Fig.4.8-4.9). The linear increase of frequency and voltage to the input of the motor lead to a quicker and smooth speed change with lower currents and constant high torque during the starting period.

Chapter II

FUNCTIONAL DESCRIPTION & MATHEMATICAL MODELLING

In this second chapter, before starting the mathematical modelling of the different modules individually, a brief functional description of each module has been provided for better understanding. Later on, each module of the system is expressed mathematically which is used to develop a complete time domain state space model in the next chapter.

2.1 OPTICAL SPEED ENCODER:

The digital optical speed encoder is used to convert the motor speed to a digital pulse train. It contains a light encoder and Schmitt trigger as shown in Fig.2.1. The light encoder consists of a disk mounted on a motor shaft with a number of holes on the perimeter and an opto-electronic emitter detector assembly. The output from the photo-transistor is not a perfect square pulse train. To have the perfect digital waveform, the Schmitt trigger circuit is employed in the speed encoder.

The speed encoder generates a pulse train of frequency f_v proportional to the actual speed of the motor ω_m (radian/sec) which can be expressed as

$$V_{se} = A \text{ Sign} [\text{Sin}(N.\omega_m)] \quad (2.1)$$

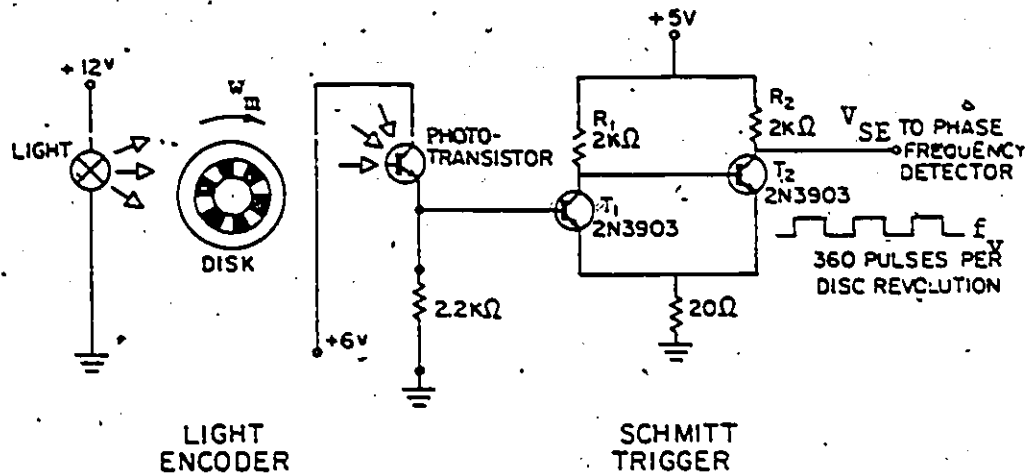


Figure 2.1 - Digital Optical Speed Encoder

$$f_v = \frac{N}{2\pi} \cdot \omega_m \quad (2.2)$$

where N is the number of holes on the disc of the encoder and $\text{Sign}(x) = 1$ for $x > 0$, and -1 for $x < 0$.

2.2 PHASE-FREQUENCY DETECTOR:

The digital phase-frequency detector (PFD) is the most crucial part of the system. It should have the following properties (i) unresponsive to the harmonics (ii) unresponsive to the change of duty cycles of the two pulse trains and (iii) wide linear operating range. A widely used sequential PFD is shown in Fig. 2.2 which has the above mentioned properties. It consists of four flip-flops plus additional logic and is available in several versions as a single chip IC. Its active phase range is $\pm 360^\circ$ which is double that of other phase detectors. The PFD characteristic is linear and aperiodic over the entire range (Fig. 2.2).

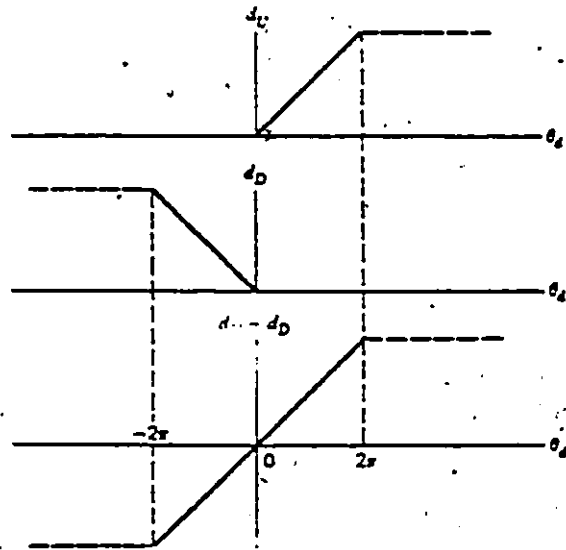
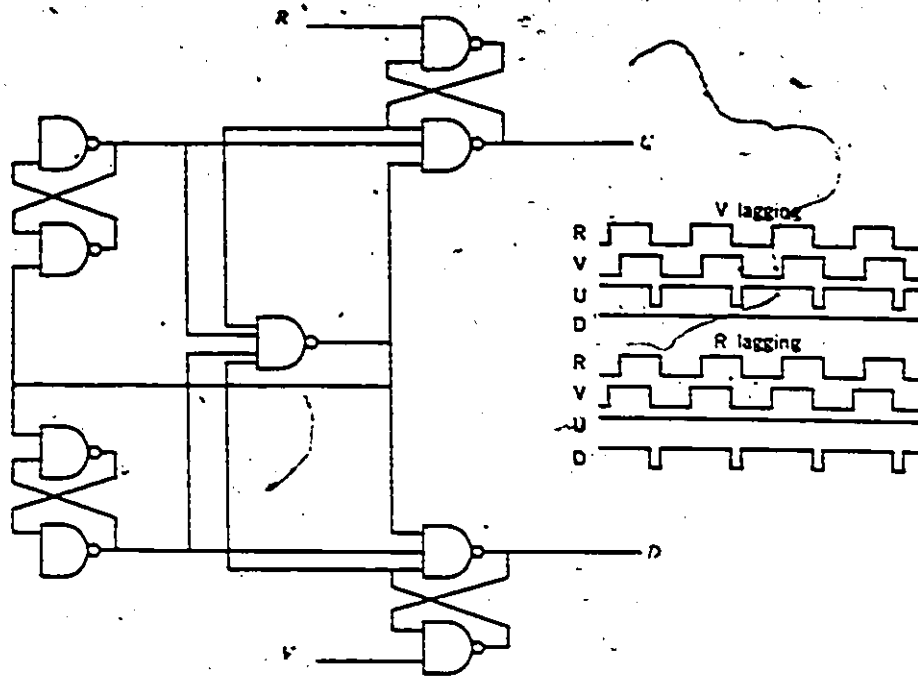


Figure 2.2 - Digital Phase-Frequency Detector and its Characteristic

Operation of the circuit can be analysed by examining the 12 different logic states possible and the transitions between the states caused by the two inputs R and V. In the unlocked conditions, the analysis indicates that one terminal (U or D depending upon the sign of the frequency

difference). will remain high as long as the loop is out of lock and the other terminal switches back and forth between levels in a manner determined by the frequency and phase difference. The detector provides an average dc signal to the loop filter when out of lock.

The detector output voltage V_e is proportional to the frequency difference between the two pulse trains (feed back and reference). Its output is composed of a DC component and harmonics. These harmonics are eliminated by the loop filter used in the system. Therefore, the detector output can be expressed simply by

$$V_e = 2\pi D_1 (f_v/f_R - 1) \quad (2.3)$$

2.3. FILTER:

The basic function of the loop filter is to remove the (undesired) harmonics from the detector output error voltage (V_e). But it also plays a significant role in determining the stability and dynamic performance of the system. Its selection is usually made on the basis of desired performance of the system. Here a very common first order active filter as shown in Fig.2.3, is used which can be easily modelled as

$$V_f = -(R_2/R_1) V_e - (1/R_1 C) \int_0^t V_e dt \quad (2.4)$$

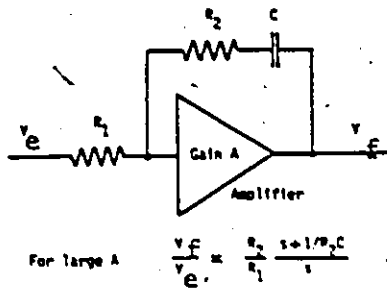


Figure 2.3 - Active Loop Filter

This filtered output is then amplified to get the appropriate level of voltage required for changing both dc output of the controlled rectifier V_d and frequency f_{co} of the VCO.

2.4 DIGITAL VOLTAGE CONTROLLED OSCILLATOR:

The digital VCO, as shown in Fig. 2.4, is an astable multivibrator with variable resistor R (using N-channel unijunction transistor) whose frequency is a function of filtered error voltage V_f . The value of R varies approximately between 1K ohms to R_1 (10K ohms). These limits are determined by the parallel combination of R_1 and the N-channel MOS device resistance R_v (which varies from about 1K ohms when fully ON to about 10^9 ohms when fully OFF).

The oscillator central frequency (ω_c) can be varied by adjustment of capacitor Cx. The time period of the pulse train of the VCO is given by

$$T = -RC \ln \left[\frac{V_{tr}}{(V_{dd} + V_{tr})} + \ln \frac{(V_{dd} - V_{tr})}{2V_{dd} - V_{tr}} \right]$$

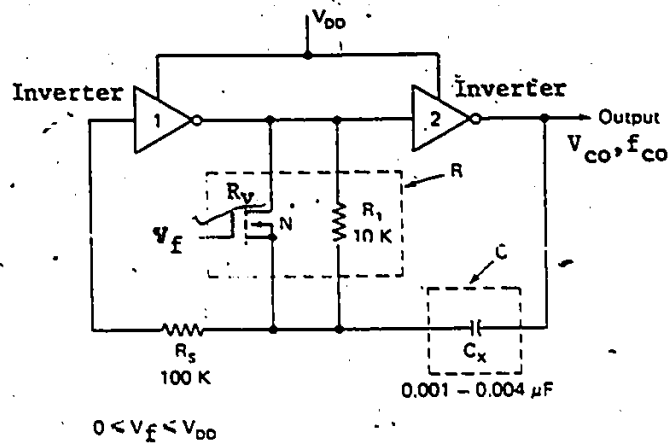


Figure 2.4 - Digital Voltage Controlled Oscillator

where $R = R_v \parallel R_1$, $C = C_x$ and V_{dd} and V_f are dc supply voltage to the VCO and transfer voltage level respectively.

The VCO is used to generate a pulse train of frequency f_{co} which is proportional to the filtered error voltage amplitude. The generated digital pulse train is used to drive the gates of the thyristors of the VSI. The pulse train of the VCO can be represented as follows

$$V_{co} = B \text{ Sign} \left[\sin(\omega_c t - k_2 \int_0^t V_f dt) \right] \quad (2.5)$$

$$f_{co} = 1/2\pi \left[d/dt (\omega_c t - k_2 \int_0^t V_f dt) \right] \quad (2.6)$$

where ω_c is the central angular frequency of VCO.

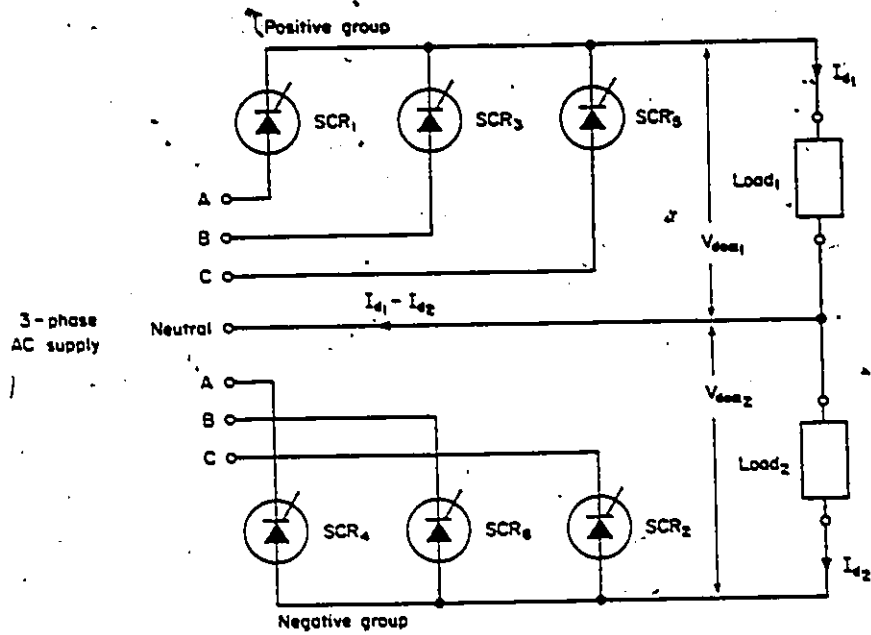
2.5 PHASE CONTROLLED RECTIFIER & TRIGGERING CIRCUIT :

2.5.1 Three Phase-controlled Rectifier

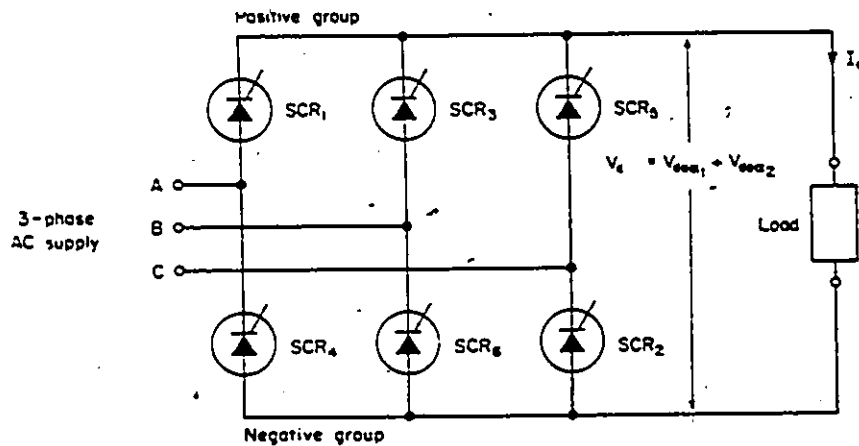
The basic function of a phase controlled rectifier is to convert an AC input voltage (60Hz) to a variable DC output voltage. The three phase-controlled rectifiers are line or self commuted ac-dc converters that produce a variable dc output voltage whose magnitude is varied by phase control, that is, by controlling the duration of the conduction period by varying the point at which a gate signal is applied to the rectifying device (thyristor). These converters are also known as six pulse converters because of six times ripple frequency of ac supply frequency. The circuit configuration and working principle is almost the same as that of a three-phase full-wave bridge rectifier except diodes are replaced by the SCR's and the dc output is adjustable by phase control.

Phase Control:

"Phase control is the process of rapid ON-OFF switching which connects an AC supply to a load for a controlled fraction of each cycle. This is a highly efficient means of controlling the average power to loads. Control is accomplished by governing the phase angle of the AC wave at which the thyristor is triggered (ON). The thyristor will then conduct for the remaining period of the cycle and OFF by phase commutation [13]."



(a)



(b)

Figure 2.5 - Three Phase-Controlled Rectifier

The six-pulse bridge converter consists of two three-pulse midpoint converters connected in series, as shown in Fig.2.5 (a). The currents that flow in the neutral are equal

and opposite, and as a result the neutral line becomes redundant. The converter configuration shown in Fig.2.5(b) is the result of eliminating the neutral. The load voltage V_d is the sum voltage of the half-wave outputs of the two series-connected three-pulse converters. For $\alpha = 0^\circ$ as shown in Fig.2.6(a), each thyristor carries the dc load current for 120 deg and blocks for 240 deg, and there is no dc current component in the ac line current. There must be two thyristors in conduction at the same time, although the conduction periods of the thyristors in the upper and lower groups do not occur simultaneously. The firing order for a supply phase sequence ABC would be SCR1 and SCR2, SCR2 and SCR3, SCR3 and SCR4, SCR4 and SCR5, SCR5 and SCR6 with commutation occurring alternatively in the upper and lower groups every 60 deg. For different values of α , the waveforms are shown in Fig.2.6(a)-(d). When $0^\circ < \alpha < 90^\circ$, the six-pulse bridge converter operates in the rectifying mode. When a source of negative voltage is present at the load for $90^\circ < \alpha < 180^\circ$, it operates in the inverting mode. The phase angle of the ac supply current lags the supply voltage as the firing delay angle is increased.

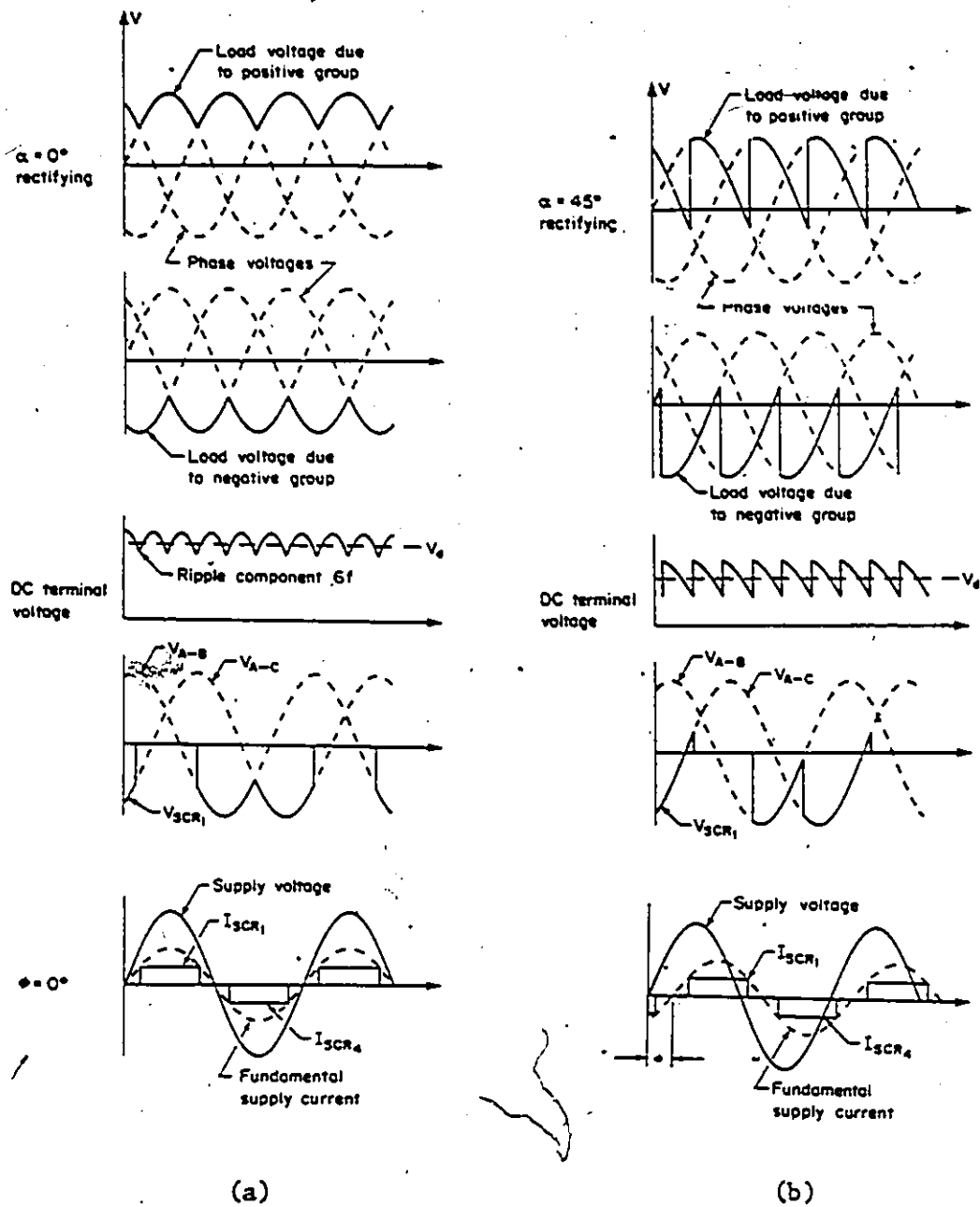


Figure 2.6 - Waveforms for Three Phase-Controlled Rectifier
 (a) $\alpha = 0^\circ$; (b) $\alpha = 45^\circ$

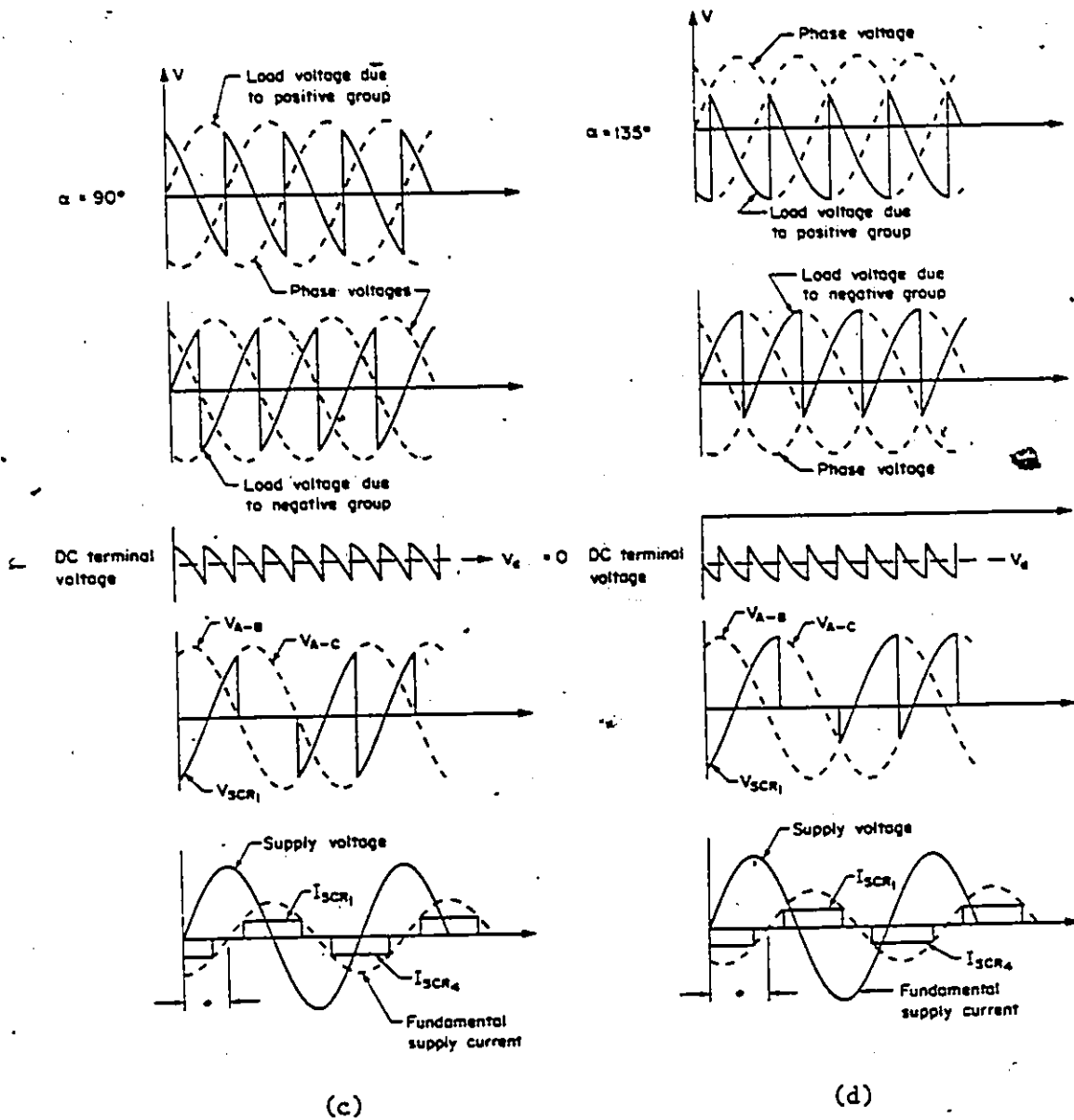


Figure 2.6(cont.) - (c) $\alpha = 90^\circ$; (d) $\alpha = 135^\circ$

The controlled rectifier output voltage, which is adjusted continuously by the change of firing angle (α) proportional to the filtered error voltage, contains a steady state d.c. component and an infinite (but converging) series of AC ripple components. In the case of the six pulse converter the frequencies of the A.C. ripples are of the order of $n=6m$ ($m=1,2,3\dots$). The output waveform, using Fourier series analysis, can be expressed [9] as

$$V_d = V_o + \sum_{n=6m}^{\infty} C_n \cos(n\omega_s t - \theta_n)$$

where

$$V_o = \frac{3}{\pi} \int_{\alpha + \pi/3}^{\alpha + 2\pi/3} V_{smax} \sin \omega_s t d(\omega_s t)$$

$$\alpha = K_3 V_f \quad (2.7)$$

$$C_n = [a_n^2 + b_n^2]^{1/2}; \quad \theta_n = \tan^{-1} a_n / b_n$$

$$a_n = \frac{6}{\pi} \int_{\alpha + \pi/3}^{\alpha + 2\pi/3} V_d \sin n \omega_s t d(\omega_s t)$$

$$b_n = \frac{6}{\pi} \int_{\alpha + \pi/3}^{\alpha + 2\pi/3} V_d \cos n \omega_s t d(\omega_s t)$$

By neglecting the higher harmonics (6th, 12th....)

$$V_d \approx \frac{3}{\pi} V_{smax} \cos \alpha \quad (2.8)$$

The phase controlled rectifier is needed in the system essentially to work at the maximum air gap flux density over the speed range of the motor for constant speed-torque characteristics. The stator voltage must be adjusted to be proportional to the frequency for constant volt/hertz ratio. Note that use of a three phase full wave rectifier in place of the phase controlled rectifier as mentioned above would result in a drooping speed-torque characteristic of the motor. This has been discussed in more detail under squirrel-cage induction motor.

2.5.2 Triggering Circuits:

For the phase control process, the triggering circuits are used to generate the current pulses of appropriate amplitude and width for triggering the thyristors efficiently and accurately. A typical circuit block diagram is shown in Fig.2.7.

A tapping from the AC supply gives the synchronized signal which is converted to a ramp waveform by using a saw-tooth generator. The ramp waveform, after a dc level shifting by the amount of error voltage, is fed to the Schmitt trigger circuit. Later these pulses are used to generate the triggering pulses for thyristor firing in a pulse shaper circuit. For proper sequence of switching of the thyristors, a logic circuit is used to steer the pulses to an appropriate thyristor through a pulse transformer for

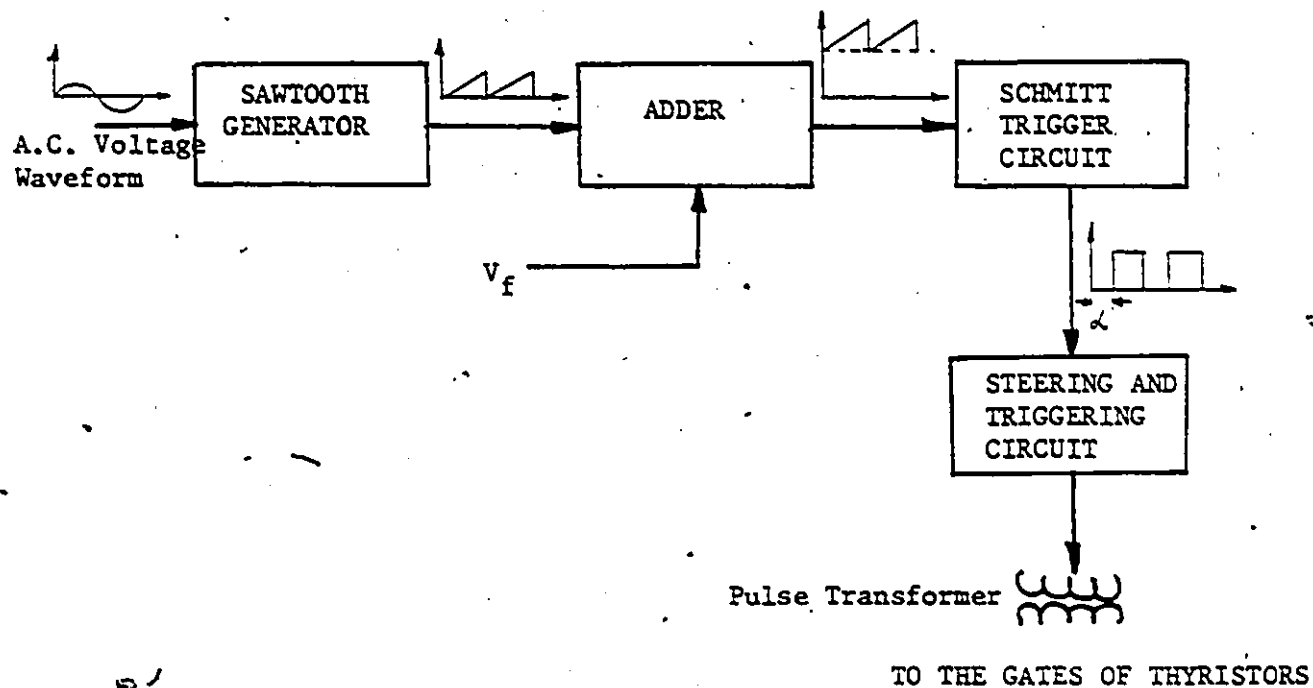


Figure 2.7 - Block Diagram of Triggering Circuit for Phase-Controlled Rectifier

isolation of control and power circuits. A sawtooth waveform enables the output of the pulse shaper to fall to zero at the same instant in every cycle but the pulse rise is phase shifted by the change of dc level (V_f) of the sawtooth waveform and hence the time when the pulse shaper switches ON. This phase shift covers nearly the whole 180° range of the cycle. By any change in the amplitude of filter voltage V_f , the position of the triggering pulses are shifted which means phase angle (α) is changed accordingly. As a result, the dc output of the phase controlled rectifier is adjusted in either direction.

2.6 VOLTAGE SOURCE INVERTER & TRIGGERING CIRCUIT :

2.6.1 Voltage Source Inverter

Basically the circuit configuration of the inverters is same as that of the controlled rectifier (as indicated in Fig.2.8(a)). Inverters convert dc power to AC power at some desired output voltage and frequency. In this case the triggering circuit is quite different and it requires a forced commutation circuit which is not required in the case of controlled rectifiers due to phase commutation of AC cycle. The frequency of the VSI output voltages can be adjusted by the frequency of the triggering pulses. The output voltage waveforms are non-sinusoidal as shown in Fig.2.8(b)-(c).

A standard McMurray three phase VSI is used to invert the dc output from the controlled rectifier into three phase AC voltages of variable frequency (proportional to filtered error voltage). Fig. 2.8(a) shows the VSI which employs auxiliary thyristors for impulse commutation. Thyristors 1 to 6 are the load carrying thyristors. They are numbered in their firing sequence. The corresponding commutating thyristors are numbered 1A to 6A.

When the load thyristors are turned ON-OFF in the correct sequence, the voltage waveforms at the three output terminals A,B,C are as shown in Fig.2.9, where the thyristor gate pulses are also shown. At any time three thyristors are

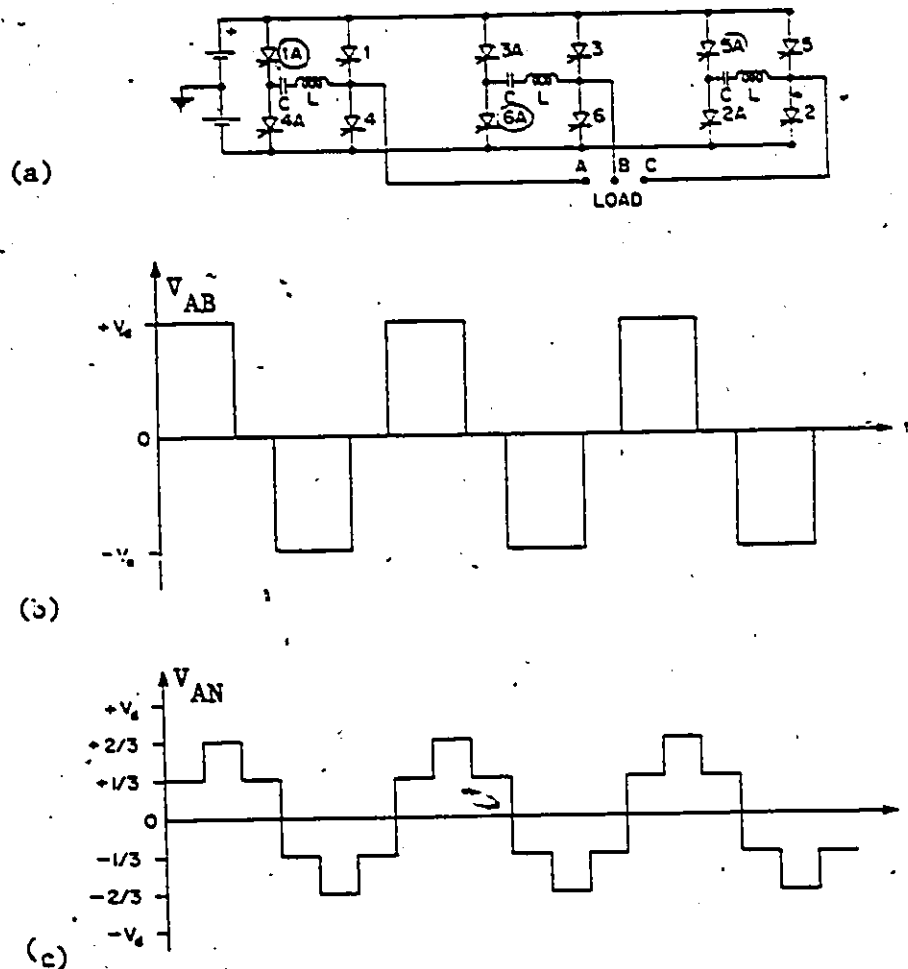


Figure 2.8 - Standard Mc Murray Voltage Source Inverter (VSI) and its output waveforms (b) Delta; (c) Star-connected Load

ON. In one cycle of the output, there should be six switching operations of the load thyristors and six of the commutation thyristors. In each phase of the inverter there are two load carrying thyristors connected in series. Only one of them should be ON at any time. The logic circuit, as discussed in the next section 2.6.2, must ensure the following (i) that one of the thyristors in a phase is prevented from conducting when the other is ON. (ii) At the

start, the correct thyristor must be triggered ON to ensure proper sequential switching in order to obtain a cyclic output. (iii) In the event of an overload all the thyristors must be turned OFF.

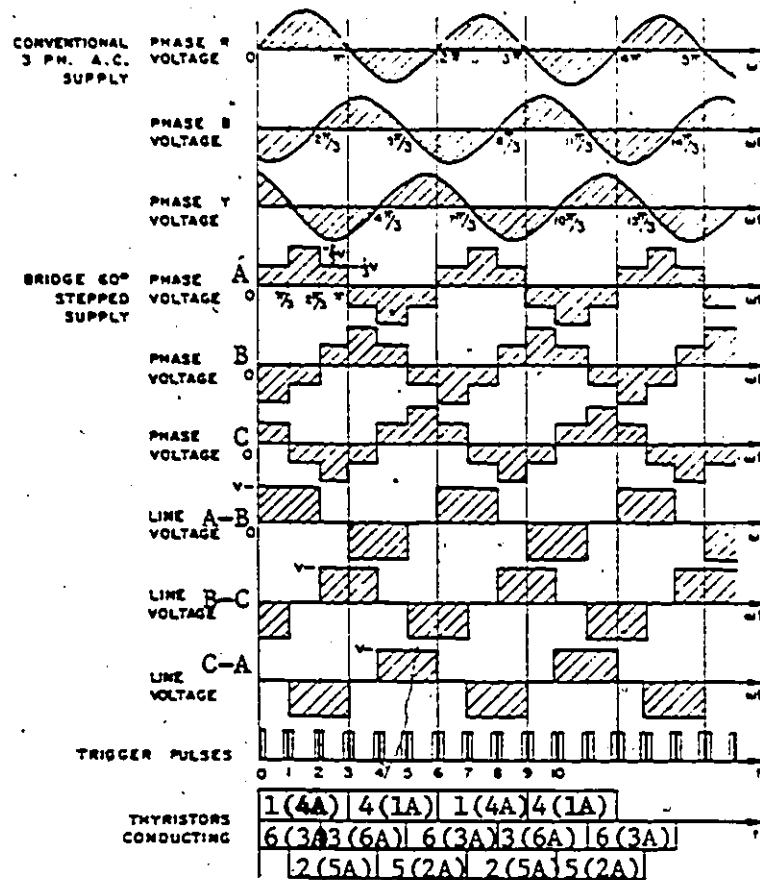


Figure 2.9 - Waveforms For Voltage Source Inverter

The VCO pulse train has been used to drive the gates of the thyristors of the VSI. The frequency of six step VSI output voltages is 1/6th of the frequency (f_{co}) of the VCO

pulse train and its output contains the harmonics of the order of $(6n+1)$ for $n=1,2,\dots$. The line-neutral voltage waveform of VSI can be expressed, using Fourier Series analysis, as follows.

$$V_{AN} = \frac{3}{\pi} V_d [\sin \omega t + 1/5 \sin 5\omega t + 1/7 \sin 7\omega t + \dots] \quad (2.9)$$

$$V_{BN} = \frac{3}{\pi} V_d [\sin(\omega t - 2\pi/3) + 1/5 \sin(5\omega t - 2\pi/3) + 1/7 \sin(7\omega t - 2\pi/3) + \dots] \quad (2.10)$$

$$V_{CN} = \frac{3}{\pi} V_d [\sin(\omega t + 2\pi/3) + 1/5 \sin(5\omega t + 2\pi/3) + 1/7 \sin(7\omega t + 2\pi/3) + \dots] \quad (2.11)$$

where

$$\omega = 1/6 (\omega_c - K_2 V_f) \quad (2.12)$$

2.6.2 Triggering and Logic Circuits:

As mentioned above, for the proper operation of the inverter a triggering and logic circuits are needed to satisfy all the conditions. A block diagram of the triggering and logic circuit is given in Fig.2.10. The digital pulse train from the VCO is fed to the ring counter which produces six output pulse trains, all separated in phase by 60° from each other.

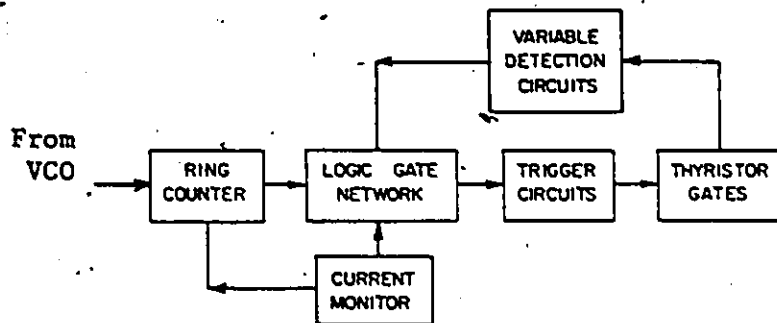


Figure 2.10 - Block Diagram of Triggering and Logic Circuit For VSI

A logic gate network is used to generate six gate pulses to the commutation thyristors 1A to 6A in desired sequence and six gate pulses to the load thyristors 1 to 6 with the sequence shown in Fig.2.9. A detail design of such triggering and logic circuit has been discussed in Appendix I of [12]. It should satisfy all the other conditions stated in the previous section. Triggering circuits provide the current pulses of the required amplitude and width necessary for the thyristor firing and isolates power and control circuits.

2.7 SQUIRREL CAGE INDUCTION MOTOR:

Induction motors are relatively cheap and rugged machines because they can be built without slip-ring or commutators. Consequently much attention has been given to the study of

Induction motor control for starting, braking, speed reversal and speed change etc.

In the induction motor, the rotor winding is short circuited and receives its supply by induction from the stator. The stator carries a three phase winding which is directly connected to a three phase AC supply. This establishes a rotating air-gap magnetic field of constant amplitude which rotates at synchronous speed n_1 .

$$n_1 = 120 f/P \quad (2.12a)$$

where P is number of poles and f is the stator supply frequency.

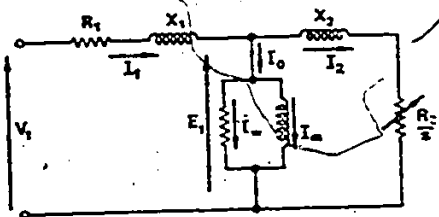


Figure 2.11 - Single Phase Equivalent Circuit of Induction Motor

The synchronous speed of the motor can, therefore, be controlled by variation of the stator supply frequency f . The amplitude of the air-gap flux is determined by the

stator volts/Hz which is explained later. When the induction motor is supplied at fixed voltage and frequency, the air-gap flux is approximately constant for all normal loading conditions. The phase sequence of the stator supply determines the direction of rotation of the air-gap field and hence determines the rotation of the motor. The motor runs at a speed, n , which is usually only a few per-cent less than the synchronous speed, n_1 . As a result, the rotor e.m.f. is at a frequency $f_2 = sf$, where the fractional slip,

$$s = f_2/f = (n_1 - n)/n_1. \quad (2.12b)$$

The rotor current, I_2 , lags the e.m.f. by the rotor phase angle, ϕ_2 , and the motor torque is proportional to the in-phase rotor current $I_2 \cos \phi_2$. The output torque is also proportional to the air-gap flux Φ , and hence,

$$T_e = K \Phi I_2 \cos \phi_2. \quad (2.12c)$$

where K is a constant of proportionality.

2.7.1 Steady State Performance:

The steady-state performance of the induction motor is analysed by means of the fundamental equivalent circuit shown in Fig, 2.11.

Constant Volts/Hz Ratio:

For normal Sin-wave operation, the skin effect is usually neglected and hence the resistances are independent of frequency, while the reactances are proportional to frequency. The rotating flux wave in the air-gap induces a counter e.m.f. E_1 in the stator winding. This e.m.f. is less than the applied voltage V_1 due to the voltage drop in $(R_1 + jX_1)$, the stator leakage impedance. Since the presence of space harmonic m.m.f. wave is ignored, the rotating flux wave has a sinusoidal space distribution, and the flux linking each stator turn has a sinusoidal time variation. If Φ denotes the flux per pole of the rotating field, the instantaneous flux linking a full span of stator turn is

$$\phi = \Phi \sin \omega t$$

where $\omega = 2\pi f$, the angular frequency of the supply voltage. The induced e.m.f. per turn is therefore

$$e_1 = d\phi/dt = \omega \Phi \cos \omega t$$

and the r.m.s phase e.m.f. is given by

$$E_1 = \omega \Phi K_w N_1 / \sqrt{2} = 4.44 K_w f N_1 \Phi \quad (2.12d)$$

where N_1 is the number of series turns per phase and K_w is the winding factor.

For constant torque and effective utilisation of the machine the air-gap flux Φ (proportional to E_1/f) of the induction motor must be sustained at all frequencies. A constant air-gap flux is obtained when the ratio E_1/f is constant, but if the stator leakage impedance is small, then

$$E_1 \approx V_1 = A f \Phi$$

where $A = 4.44 K_v N_1$

$$\text{or } \Phi = 1/A (V_1/f) \quad (2.12e)$$

Consequently, the air-gap flux is nearly constant when the ratio V_1/f has a fixed value. This is the constant flux mode of operation which is commonly used in open loop system.

Torque-Speed:

At a slip s , the rotor power loss in the equivalent circuit (Fig.2.1f) is $I_2^2 R_2/s$ watts per phase, whereas in the actual machine the rotor copper loss is $I_2^2 R_2$ watts per phase. The additional power loss in the equivalent circuit is the electrical equivalent of the mechanical power output of the rotor. If P_m denotes the gross mechanical power output including windage and friction losses, then

$$\begin{aligned} P_m &= m_1 [I_2^2 (R_2/s) - (I_2^2 R_2)] \\ &= m_1 I_2^2 R_2 (1-s)/s \end{aligned}$$

where m_1 is the number of stator phases.

But

$$\begin{aligned} P_m &= T_e \omega_m \\ T_e &= (m_1/\omega_m) I_2^2 R_2 (1-s)/s \end{aligned}$$

$$\text{or } T_e = (P \frac{n_1}{4\pi f}) I_2^2 R_2/s \quad (2.12f)$$

Fig.2.12 shows the torque-speed characteristics of a typical cage-rotor induction motor operating on a standard fixed frequency supply.

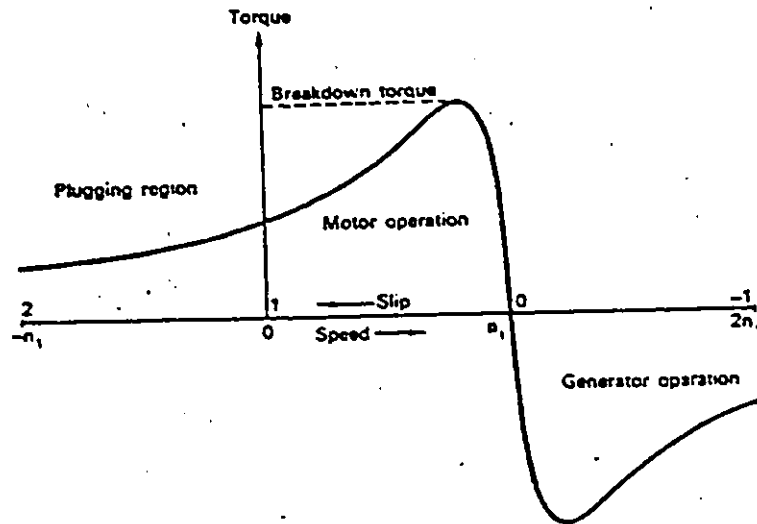


Figure 2.12 - Torque-Speed Characteristic of Induction Motor at Constant Voltage and Frequency

Motor Operation:

At synchronous speed the motor develops zero torque, and the speed decreases linearly with torque when the slip is small. The induction motor is almost a constant speed motor. As the rotor slip frequency increases, the rotor leakage reactance becomes significant and increases the rotor impedance and also the phase angle ϕ_2 . With increasing

slip, the motor torque therefore reaches a maximum and then diminishes. The maximum torque is called the breakdown torque, since the motor stalls if the load torque exceeds this peak value. The rotor frequency at the breakdown point is called the rotor breakdown frequency.

Plugging Operation:

If the motor rotates backwards against the forward rotating field the slip is greater than unity, and a counter-torque is developed which opposes the rotation. The motor operates in this region of the characteristic if two stator leads are suddenly reversed when the machine is operating normally as a motor. This changes the phase sequence of the stator currents and hence reverses the direction of rotation of the air-gap field. The machine is brought rapidly to rest and, if supply is not disconnected, the rotor then speeds up in the opposite direction. This method of braking or rapidly reversing the induction motor is known as Plugging.

Generator Operation:

The torque-speed curve may also be extended into the generator region, above synchronous speed. In this region, the slip is negative and the machine converts mechanical

energy at the shaft into electrical energy which is returned to the AC network. The machine operates under these conditions when the rotor is driven mechanically at super-synchronous speeds. Generation operation also occurs in a variable-frequency system when the supply frequency is rapidly reduced.

2.7.2 Adjustable Frequency Operation of Induction Motor:

As mentioned earlier, the actual speed, n , of the induction motor is less than the synchronous speed, n_1 , of the motor which can be controlled by variation of the supply frequency, f .

$$n = n_1(1-s) = 120f(1-s)/P \quad (2.12g)$$

The relation (2.12g) shows that the induction motor could be used as an adjustable speed drive with the variable-frequency static power supply. Basically the inverter releases the AC machine from its inherent limitation of being used only in single speed drive applications.

From the equivalent circuit Fig.2.11, the rotor current I_2 is defined by

$$I_2 = \frac{E_2}{[R_2^2 + (sX_2)^2]^{\frac{1}{2}}} = \frac{E_1}{[(R_2/s)^2 + X_2^2]^{\frac{1}{2}}} \approx \frac{V_1}{[(R_2/s)^2 + X_2^2]^{\frac{1}{2}}} \quad (2.12h)$$

and rotor slip $s = f_2/f$ (2.12i)

The torque equation (2.12f) can be written using above equations as follows

$$T_e = \frac{P_m}{4\pi} [V_1/f]^2 [f_2 R_2 / (R_2^2 + 4\pi^2 \frac{1}{2} L_2^2)] \quad (2.12j)$$

By maximizing the torque equation (2.12j), an expression for the breaking torque and breaking rotor frequency are obtained as shown below

$$T_b = \pm \frac{P_m}{4\pi} [V_1/f]^2 1/4\pi L_2 \quad (2.12k)$$

$$\text{and } f_{2b} = \pm R_2 / 2\pi L_2 \quad (2.12l)$$

Fig.2.13 shows the torque characteristics of the motor at several different stator frequencies. The breakdown torque is maintained constant by adjusting the stator volts/Hz, so that the air-gap flux is constant. These motor characteristics are suitable for driving a constant-torque load at variable speed in open loop and constant speed at variable load in closed loop. The supply frequency and voltage are corrected in real time according to the actual speed.

At very low frequencies, however, the induction motor torque decreases considerably. This is caused by the reduction in air-gap flux at low frequency due to the increased influence of the stator resistance. The stator resistance voltage drop at rated current has the same magnitude at all frequencies, and it therefore constitutes a considerably higher fraction of the supply voltage at low frequency than at rated frequency when it may often be neglected. Fig. 2.14 shows the break-down and starting

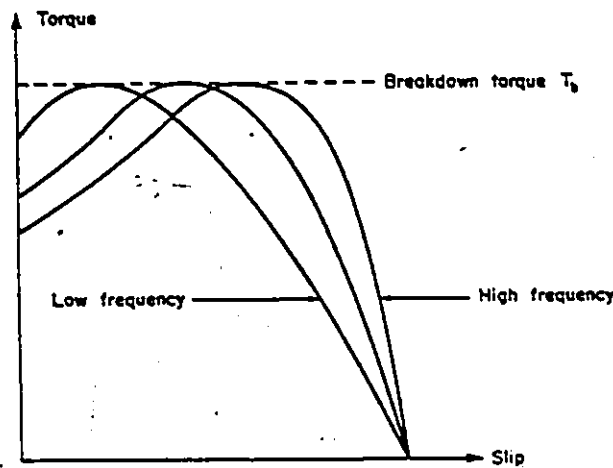
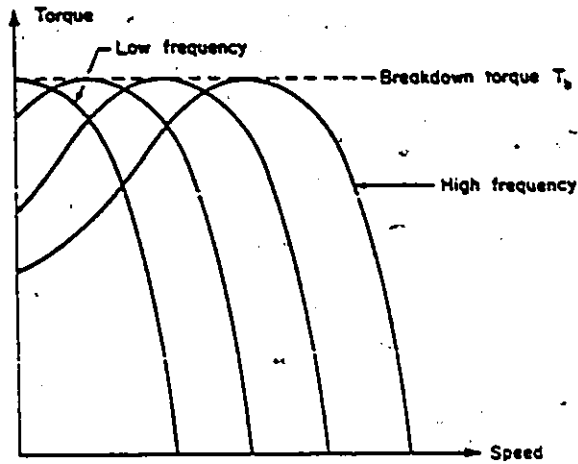


Figure 2.13 - Torque-Speed and Torque-Slip Characteristics at different supply frequencies and constant air-gap flux

torque vs stator frequency. There is a serious reduction in both of these torques at frequencies less than 10 Hz. To improve the low frequency performance characteristics, the terminal voltage should be increased considerably about its frequency - proportional value. This can be easily done in such systems due to independent adjustments of output voltage and frequency.

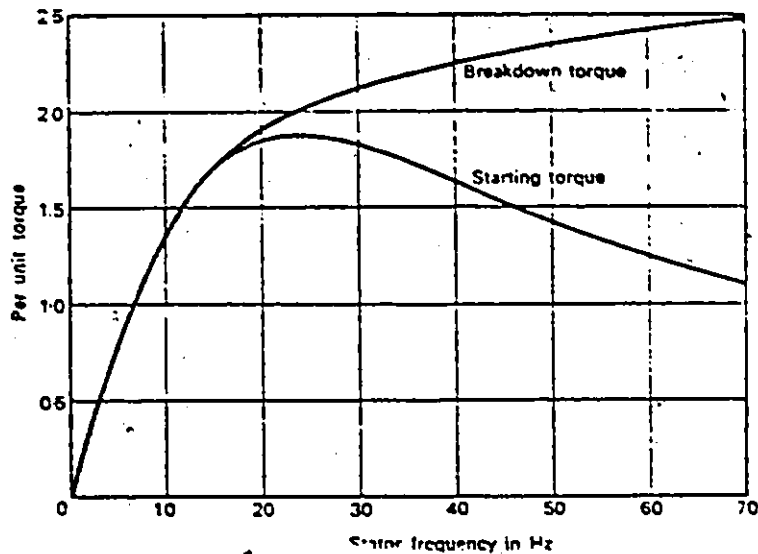


Figure 2.14 - Break-down and Starting Torque Vs Stator Frequency Characteristics.

On the other hand to avoid this problem, if the stator voltage remains constant as the frequency is varied, the air-gap flux and breakdown torque decrease with increasing frequency as shown in Fig.2.15. These characteristics are suitable for traction applications where a large torque is required at standstill and low speed, and a smaller torque is sufficient for high-speed running.

The standstill current of a typical squirrel-cage induction motor is 5 to 8 times of rated current, but the starting torque is small because of low rotor power factor at high rotor frequencies. In a variable frequency system, the supply frequency is reduced for starting. This improves

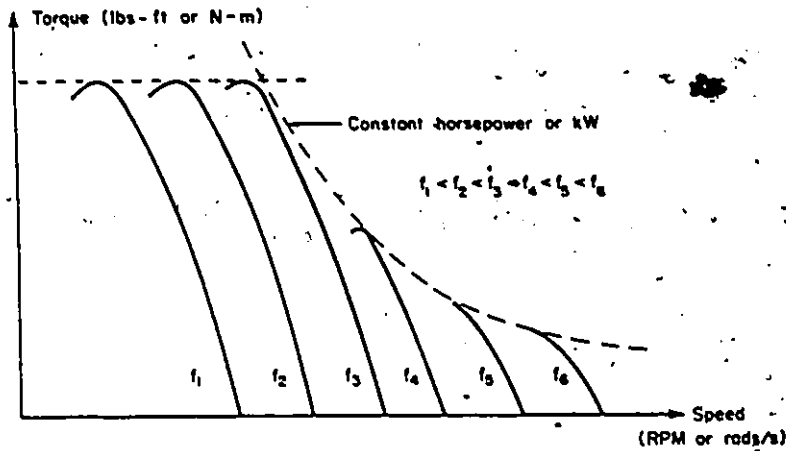


Figure 2.15 - Torque-Speed Characteristics for variable frequency operation in constant torque and constant horsepower modes

the rotor power factor and so increases the torque per ampere at starting. The air-gap flux can also be increased by adjusting the stator volts/Hz. In this manner several times rated torque is available at standstill as shown in Fig. 2.13 & 2.15, and the induction motor is rapidly run-up to speed by increasing the supply frequency. With this method of starting, there is no danger of the low-frequency crawling which some times occurs when induction motor are started on a fixed-frequency supply.

2.7.3 Mathematical Model

AC machines could be analysed in the steady state by an equivalent circuit. To study transient behavior, however, AC machines must be represented more accurately by a set of non-linear differential equations in the time domain.

A squirrel-cage induction motor can be modeled in the time domain [5] as

$$\begin{bmatrix} V_s \\ V_r \end{bmatrix} = \begin{bmatrix} R_s + L_{ss} p & (pL_{sr}) + L_{sr} p \\ (pL_{rs}) + L_{rs} p & R_r + L_{rr} p \end{bmatrix} \begin{bmatrix} I_s \\ I_r \end{bmatrix} \quad (2.13)$$

where

$$V_s = [V_{AN}, V_{BN}, V_{CN}]', \quad V_r = [0, 0, 0]'$$

$$R_s = \begin{bmatrix} r_1 & 0 & 0 \\ 0 & r_1 & 0 \\ 0 & 0 & r_1 \end{bmatrix}, \quad R_r = \begin{bmatrix} r_2 & 0 & 0 \\ 0 & r_2 & 0 \\ 0 & 0 & r_2 \end{bmatrix}$$

$$L_{ss} = L_{rr} = L_a \begin{bmatrix} 1 & \cos 2\pi/3 & \cos 4\pi/3 \\ \cos 2\pi/3 & 1 & \cos 2\pi/3 \\ \cos 2\pi/3 & \cos 4\pi/3 & 1 \end{bmatrix}$$

and

$$L_{sr} = L_{rs}' = M \begin{bmatrix} \cos \theta & \cos(\theta + 2\pi/3) & \cos(\theta - 2\pi/3) \\ \cos(\theta - 2\pi/3) & \cos \theta & \cos(\theta + 2\pi/3) \\ \cos(\theta + 2\pi/3) & \cos(\theta - 2\pi/3) & \cos \theta \end{bmatrix}$$

The internal electrical torque T_e developed by the motor is

$$T_e = (P/2) 1/2 [I_s \ I_r] \begin{pmatrix} L_{ss} & L_{sr} \\ L_{rs} & L_{rr} \end{pmatrix} \begin{bmatrix} I_s \\ I_r \end{bmatrix} \quad (2.14)$$

and the mechanical torque equation of the motor and load is given by

$$T_e = T_L + Jp\omega_m + K\omega_m \quad (2.15)$$

$$\dot{\theta} = (P/2)\omega_m \quad (2.16)$$

Chapter III

DEVELOPMENT OF TIME DOMAIN STATE SPACE MODEL

Generally, for efficient computation, AC drive systems are analysed using the d-q transformation which holds only under certain assumptions [8] (e.g. balanced and symmetrical system, absence of any harmonics etc.). However, when these assumptions are not valid, the d-q transformation can not be applied. Therefore, a time domain model (without d-q transformation) has been developed for the adjustable & precise speed-controlled AC drive system.

For complete dynamics of the system (Fig.1.2), the mathematical representation of each block, equations(2.1-2.16), are rewritten for the convenience as follows

$$\begin{bmatrix} V_s \\ V_r \end{bmatrix} = \begin{bmatrix} R_s + L_{ss} P & (PL_{sr}) + L_{sr} P \\ (PL_{rs}) + L_{rs} P & R_r + L_{rr} P \end{bmatrix} \begin{bmatrix} I_s \\ I_r \end{bmatrix}$$

$$T_e = (P/2) 1/2 [I_s \ I_r] \begin{pmatrix} L_{ss} & L_{sr} \\ L_{rs} & L_{rr} \end{pmatrix} \begin{bmatrix} I_s \\ I_r \end{bmatrix}$$

$$T_e = T_L + Jp\omega_m + K\omega_m$$

$$\dot{\theta} = (P/2) \omega_m$$

$$V_{se} = A \text{ Sign} [\text{Sin}(N \cdot \omega_m)]$$

$$f_v = \frac{N}{2\pi} \omega_m$$

$$V_e = 2W D_1 (f_v / f_R - 1)$$

$$\begin{aligned} V_f &= (-R_2/R_1)V_e - (1/R_1C) \int_0^t V_e dt \\ V_{co} &= B \text{ Sign} [\sin(\omega_c t - k_2 \int_0^t V_f dt)] \end{aligned} \quad (3.1)$$

$$f_{co} = 1/2\pi [d/dt(\omega_c t - k_2 \int_0^t V_f dt)]$$

$$V_d = 3/\pi V_{smax} \cos \alpha$$

$$\alpha = K_3 V_f$$

$$V_{AN} = \frac{3}{\pi} V_d [\sin \omega t + 1/5 \sin 5\omega t + 1/7 \sin 7\omega t + \dots]$$

$$V_{BN} = \frac{3}{\pi} V_d [\sin(\omega t - 2\pi/3) + 1/5 \sin(5\omega t - 2\pi/3) + 1/7 \sin(7\omega t - 2\pi/3) + \dots]$$

$$V_{CN} = \frac{3}{\pi} V_d [\sin(\omega t + 2\pi/3) + 1/5 \sin(5\omega t + 2\pi/3) + 1/7 \sin(7\omega t + 2\pi/3) + \dots]$$

$$\omega = 1/6 (\omega_c - K_2 V_f)$$

Now from the above mathematical representation of the system, equation (3.1), the following time domain state space model is obtained

$$\begin{cases}
 \dot{I}_s = -L_{ss}^{-1} [R_s I_s + p(L_{sr} I_r)] + L_{ss}^{-1} V_s \\
 \dot{I}_r = -L_{rr}^{-1} [p(L_{rs} I_s) + R_r I_r] + L_{rr}^{-1} V_r \\
 \dot{w}_m = \frac{1}{J} p I' [L(\theta)]_{\theta} I - \frac{K}{J} w_m - \frac{T}{J} \\
 \dot{\theta} = \frac{p}{2} w_m \\
 \dot{V}_e = 2\pi K_1 \left\{ \frac{1}{J} \frac{p}{4} I' [L(\theta)]_{\theta} I - \frac{K}{J} w_m - \frac{T}{J} \right\} \\
 \dot{V}_f = 2\pi K_1 K_4 \left\{ \frac{1}{J} \frac{p}{4} I' [L(\theta)]_{\theta} I - \frac{K}{J} w_m - \frac{T}{J} \right\} + K_5 V_e
 \end{cases} \quad (3.2)$$

where

$$I = [I_s \ I_r]'; \quad [L(\theta)]_{\theta} = \frac{\partial}{\partial \theta} \begin{bmatrix} L_{ss} & L_{sr} \\ L_{rs} & L_{rr} \end{bmatrix}; \quad K_1 = D_1 N / 2\pi f_R \\
 V_r = [0, 0, 0]' \text{ for SIM}; \quad K_4 = -R_2 / R_1; \quad K_5 = -1 / R_1 C$$

The feedback control V_s can be written in the following

form

$$V_s = [v^0, v^1, v^{+1}]' \quad (3.3)$$

where

$$v^k = \left(\frac{3}{\pi} \right)^2 v_{smax} \cos(K_3 w) \left[\sin(\omega t + 2\pi K / 3) + \sum_{n=1}^{\infty} \sum_{m=1}^2 \left\{ \sin[(6n + (-1)^m] \omega t + 2\pi K / 3] \cdot 1 / (6n + (-1)^m) \right\} \right]$$

for $K=0, -1, +1$.

and $w = 1/6 (\omega_c - K_2 V_f)$

For convenience of representation, the complete system model can be written in the state space form as follows:

$$\begin{cases}
 \dot{x} = F(x, u, t) & , t > 0 \\
 u = G(x, t)
 \end{cases}$$

where

$$x = [I_s, I_r, w_m, \theta, V_e, V_f]'; \quad \text{and} \quad u = V_s$$

The function F is derived from the right hand side of equation (3.2) and G from equation (3.3).

The complete dynamics of the system could be presented mathematically in matrix form as follows, using state space equation (3.2) and feed-back control (3.3). The matrix representation gives an overall view of the system dynamics.

$$\dot{x} = [A(x,t)]x + [B(x,t)]u \quad (3.4)$$

where

$x = [I \ \omega_m \ \theta \ V_e \ V_f]^T$, I is a six dimensional column vector and is defined as $I = [I_s \ I_r]^T$

$u = [V \ 1 \ 0 \ 1 \ 1]^T$, V is a six dimensional column vector and can be defined using equation (3.3):

$$V = [V_s \ V_r]^T = [V^0, V^{-1}, V^{+1}, 0, 0, 0]^T$$

$$[A] = \begin{bmatrix} A_{11} & A_{12} & A_{13} & A_{14} & A_{15} \\ A_{21} & -K/J & 0 & 0 & 0 \\ A_{31} & P/2 & 0 & 0 & 0 \\ A_{41} & -2\omega K_1 K/J & 0 & 0 & 0 \\ A_{51} & -2\omega K_1 K_4 K/J & 0 & K_5 & 0 \end{bmatrix}$$

In the first row of matrix [A], A_{12} , A_{13} , A_{14} and A_{15} are six dimensional column vectors of zero elements. And A_{11} is a

six dimensional square matrix which can be defined as follows

$$A_{11} = -\bar{L}^{-1} [R + dL/dt]$$

where

$$R = \begin{bmatrix} R_s & 0 \\ 0 & R_r \end{bmatrix}$$

$$L = \begin{bmatrix} L_{ss} & L_{sr} \\ L_{rs} & L_{rr} \end{bmatrix}$$

Here A_{21}, A_{31}, A_{41} and A_{51} are six dimensional row vectors which are given by

$$A_{21} = P/4J [I' dL/d\theta]$$

$$A_{31} = [0, 0, 0, 0, 0, 0]$$

$$A_{41} = 2\pi K_1 P/4J [I' dL/d\theta]$$

$$A_{51} = 2\pi K_1 k_4 P/4J [I' dL/d\theta]$$

and the remaining elements of the matrix [A] are scalars.

The matrix [B] is given by

$$[B] = \begin{bmatrix} B_{11} & B_{12} & B_{13} & B_{14} & B_{15} \\ B_{21} & -T_L/J & 0 & 0 & 0 \\ B_{31} & 0 & 0 & 0 & 0 \\ B_{41} & 0 & 0 & -2\pi K_1 T_L/J & 0 \\ B_{51} & 0 & 0 & 0 & -2\pi K_1 K_4 T_L/J \end{bmatrix}$$

Similarly, $B_{12}, B_{13}, B_{14}, B_{15}$ are six dimensional column vectors of zero elements and B_{11} is a six dimensional square matrix which is defined by

$$B_{11} = [L^{-1}].$$

and $B_{21}, B_{31}, B_{41}, B_{51}$ are six dimensional row vectors of zero elements. Here also, the remaining elements in the matrix [B] are scalars.

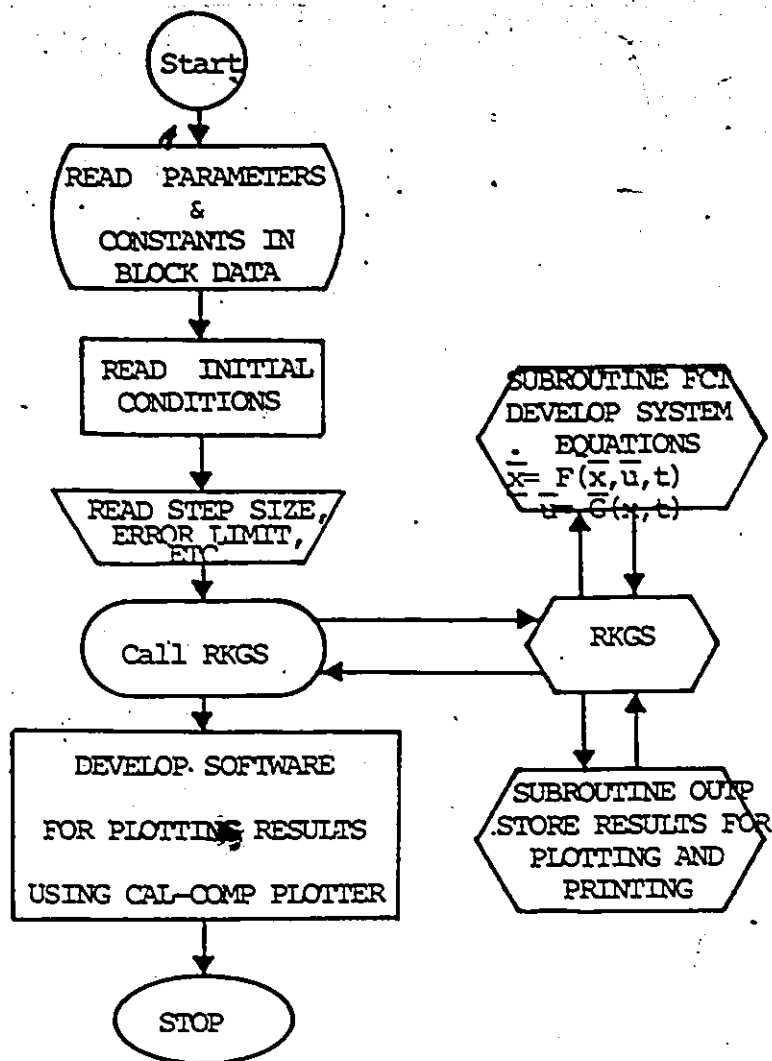
Chapter IV

DIGITAL SIMULATION & NUMERICAL RESULTS

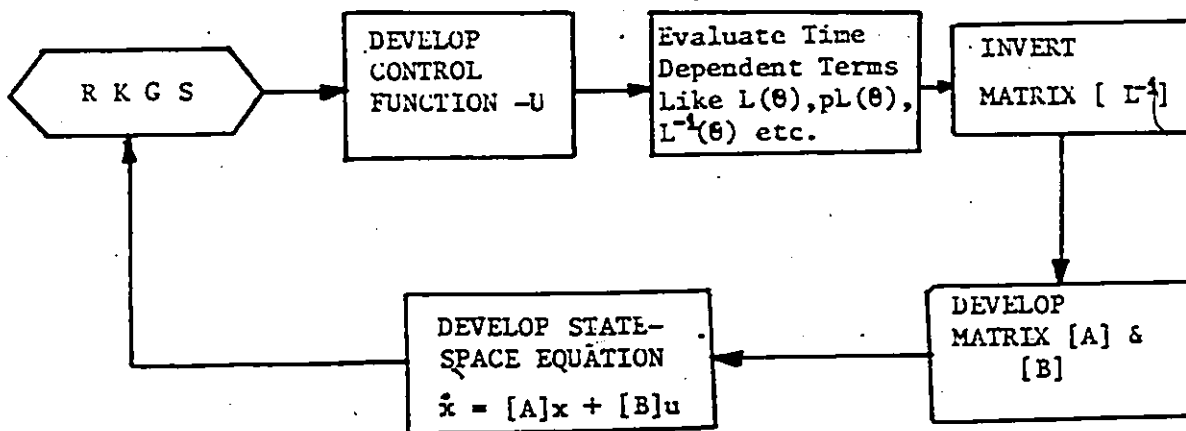
4.1 DIGITAL SIMULATION

Digital simulation, an efficient and most economical technique, is being widely used to study and analyse the performance of complex systems which are represented mathematically by a complicated set of non-linear differential equations. To see the starting transients and steady state speed-control performance of this system, the state space model equations (3.2)-(3.4) have been simulated in two different ways on University of Ottawa's Digital computer AMDAHL 470/V611. Fig.4.1 shows the flow charts used for these simulations.

Firstly, according to the flow chart as shown in Fig.4.1(a), the system has been solved by using a numerical integration method (RKGS subroutine). For better understanding and analysis this system was simulated in three ways. In the first case, only the induction motor (without any control) has been simulated while it was excited by a fixed frequency AC voltage input and the results of starting transients (current, speed, torque) including no load/full load step response were plotted using CALCOMP plotter (Fig.4.2-4.6). In the second case, the

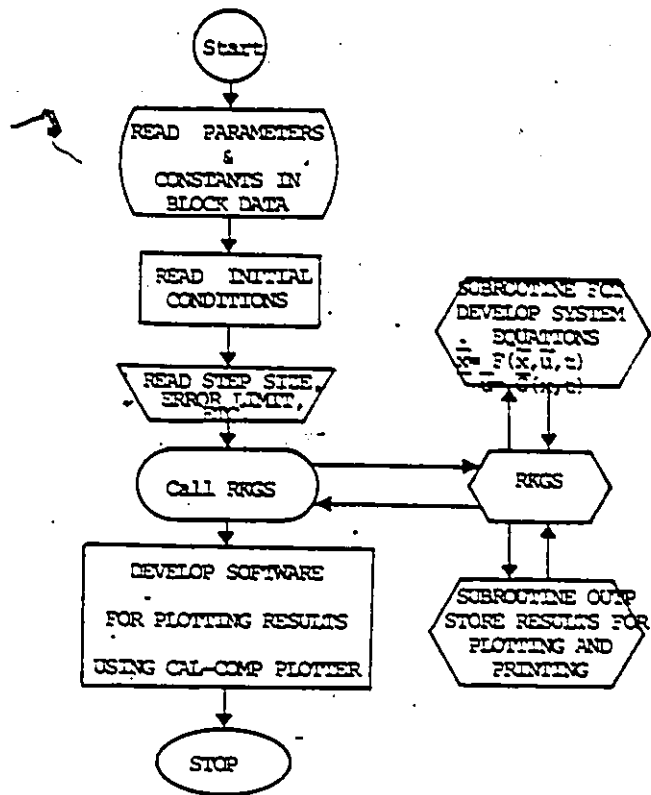


MAIN PROGRAM

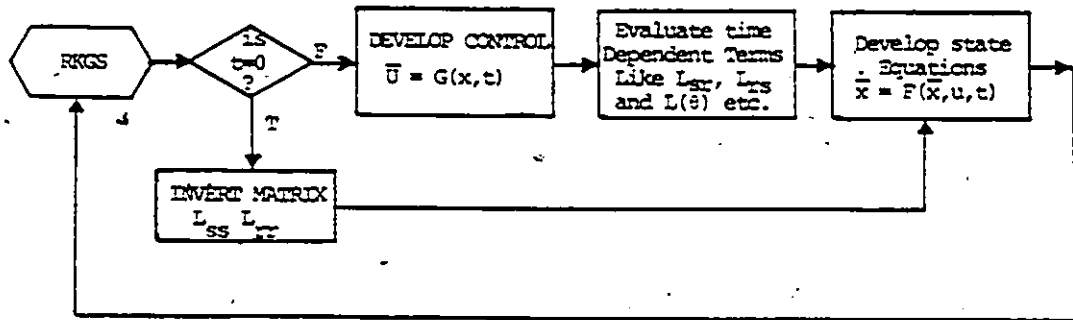


SUBROUTINE - FCI

Figure 4.1 (a) - Flow Chart For Simulation of the System With Inversion of Matrix



MAIN PROGRAM



SUBROUTINE FCT

Figure 4.1(b) Flow Chart For Simulation of the System

complete system (with control but neglecting harmonics) has been simulated and the computed results were again plotted on the same graphs. Finally, to see the effect of the harmonics of the VSI output, the system with 5th, 7th and 11th harmonics have been investigated (Fig.4.11-4.14).

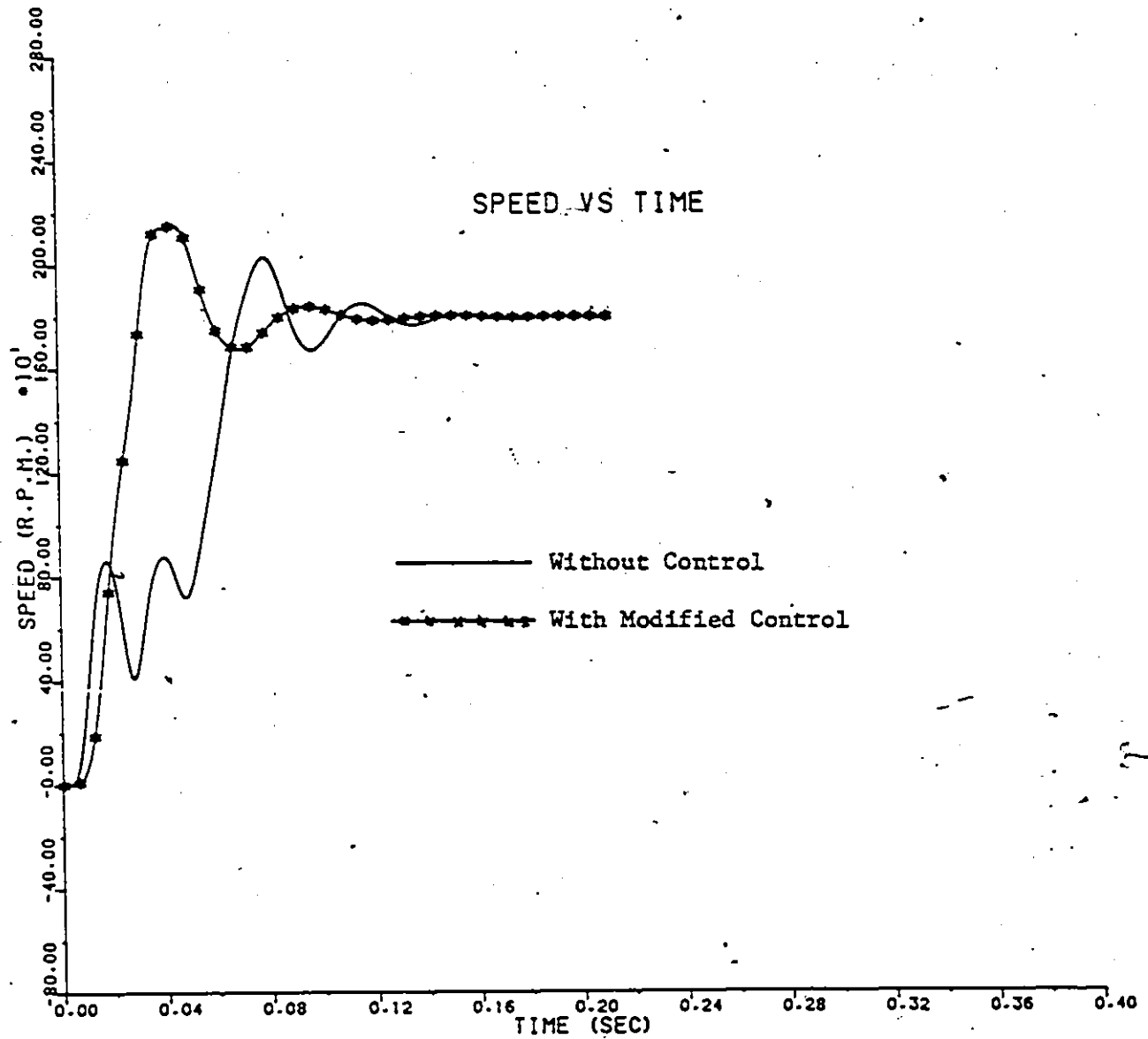


Figure 4.2 - Transient Speed Build-up during starting Without Harmonics

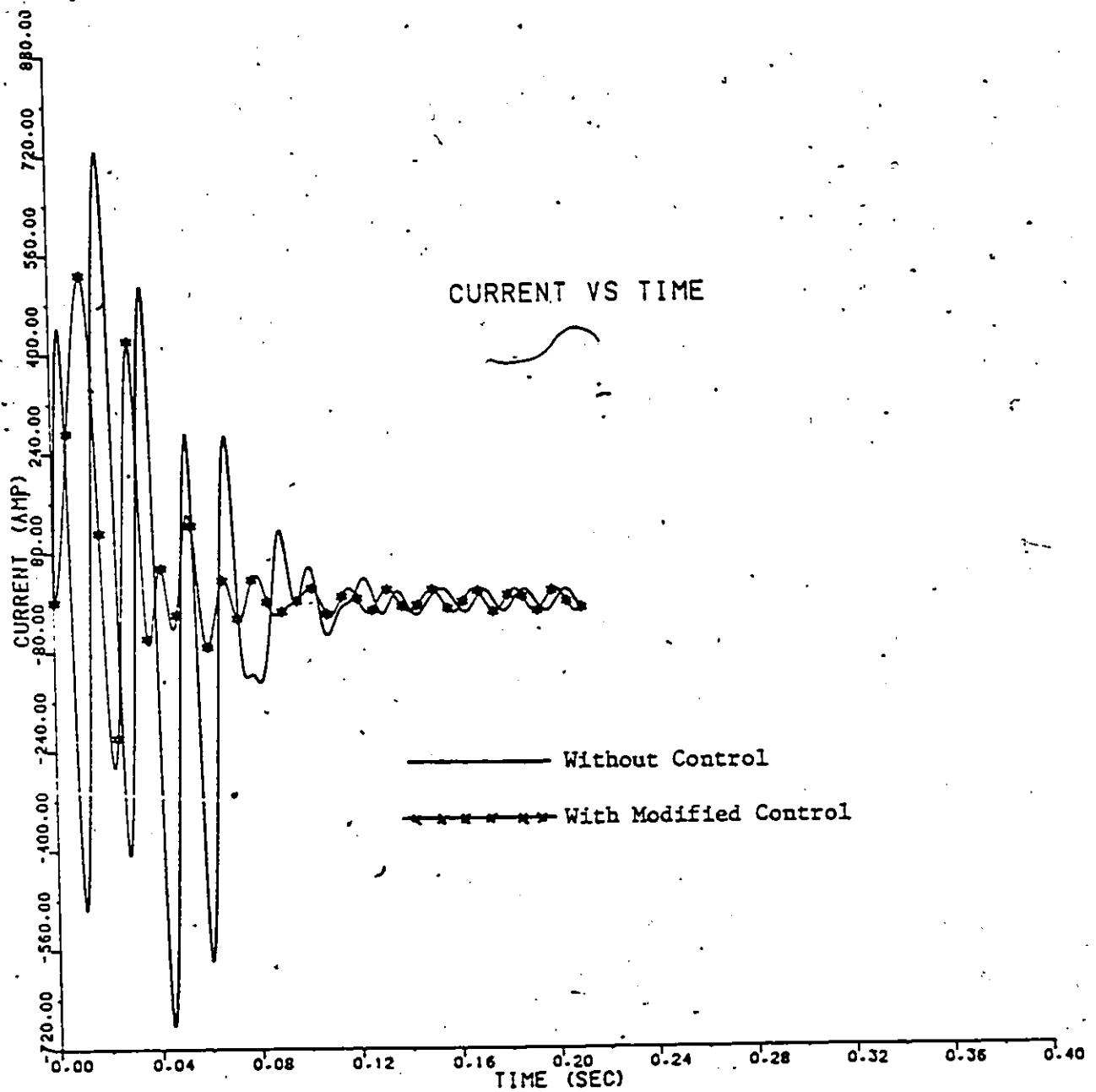


Figure 4.3 - Transient Current during Starting without harmonics

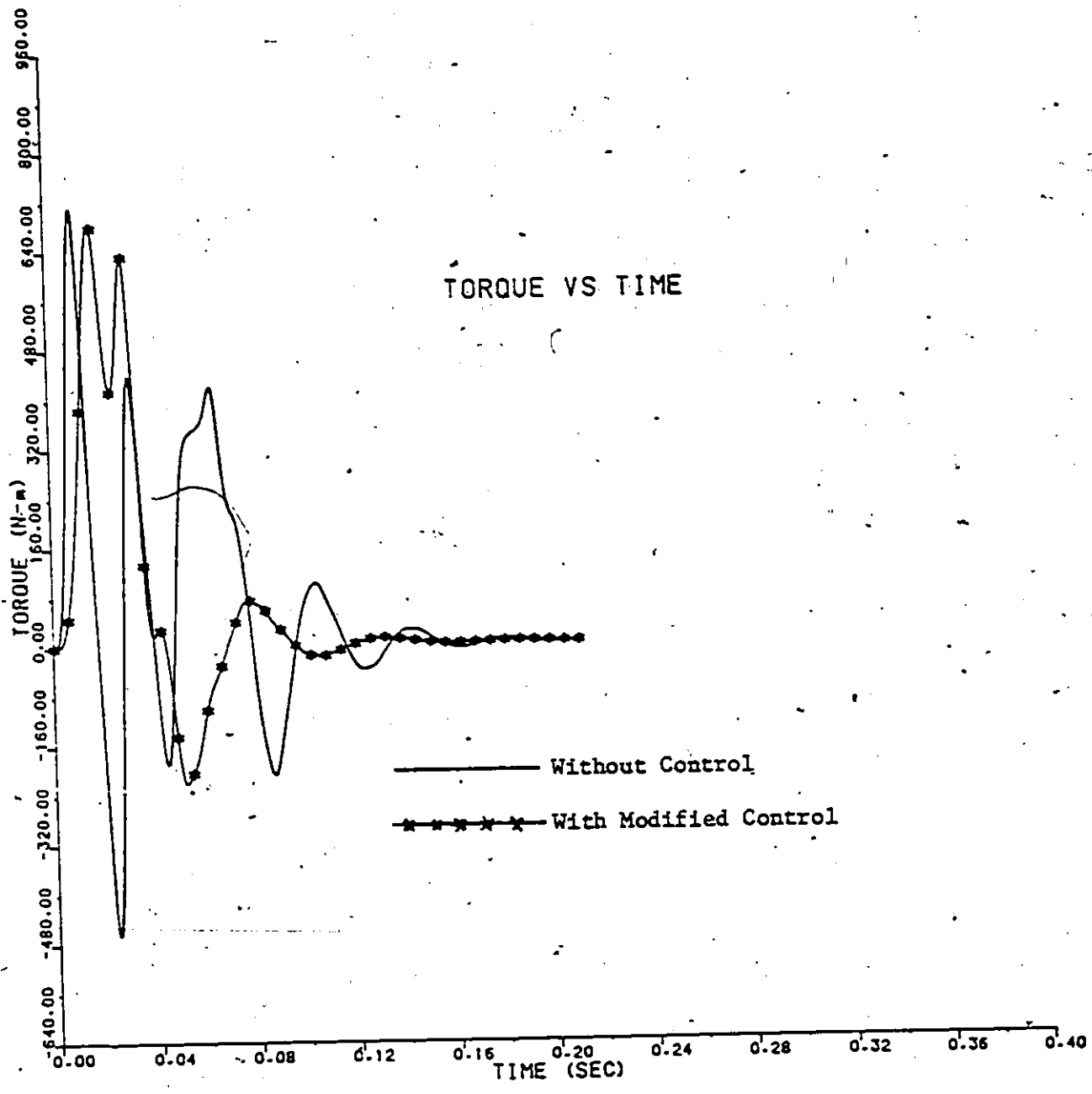


Figure 4.4 - Transient Torque-Time Characteristics during Starting Without Harmonics

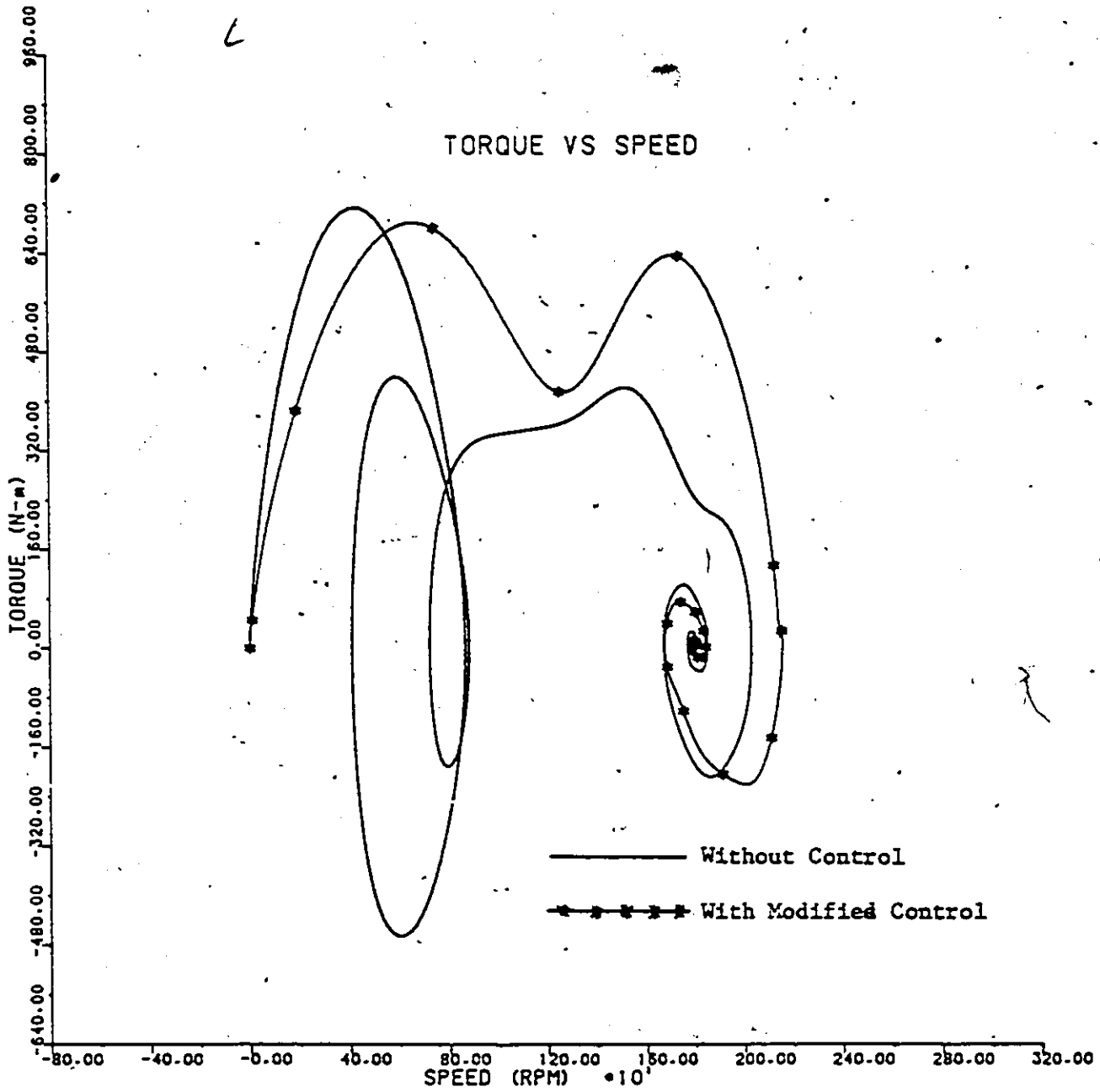


Figure 4.5 - Transient Torque-Speed Curves during Starting Without Harmonics

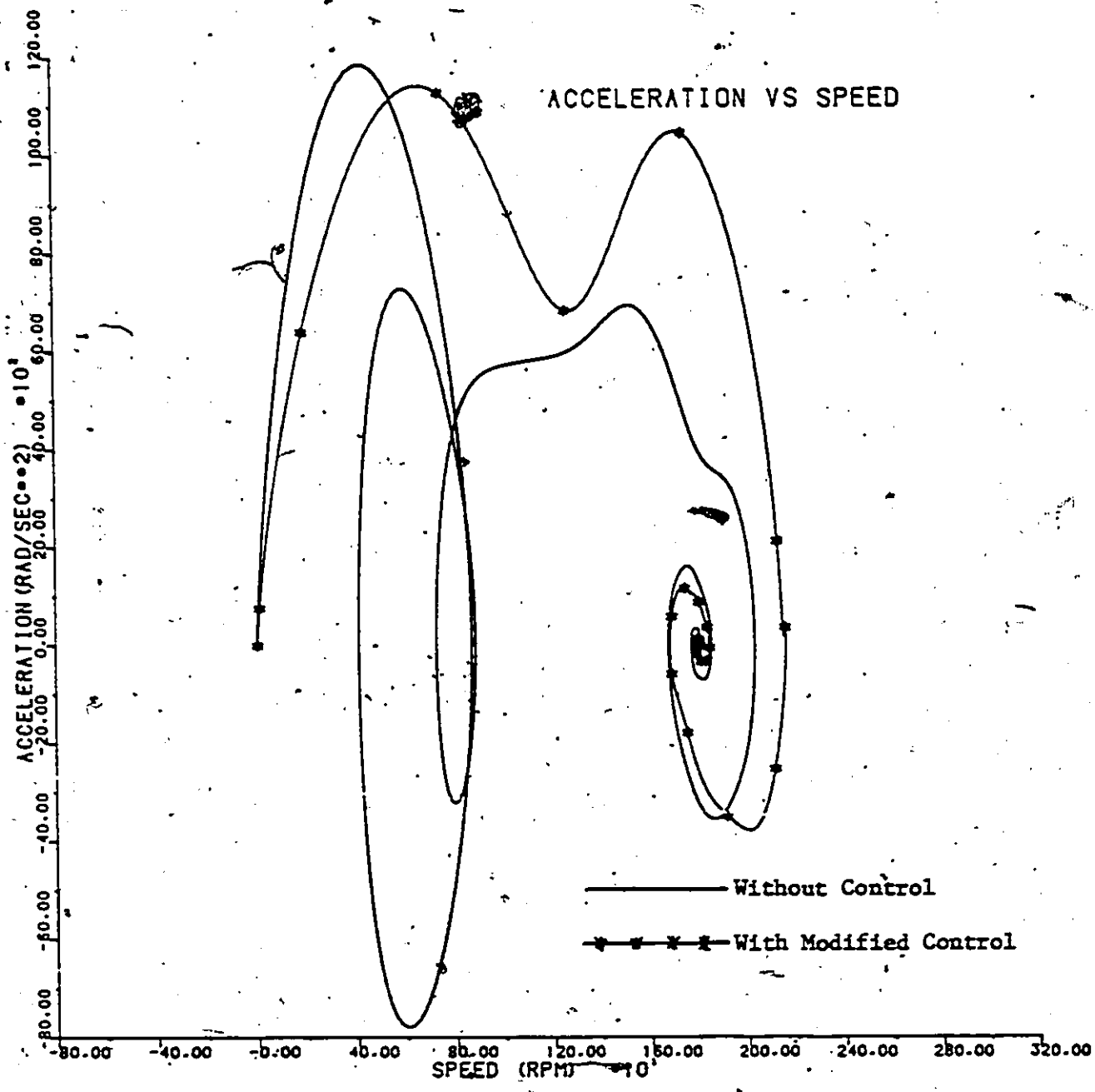


Figure 4.6 - Transient Acceleration-Speed Curves during Starting Without Harmonics

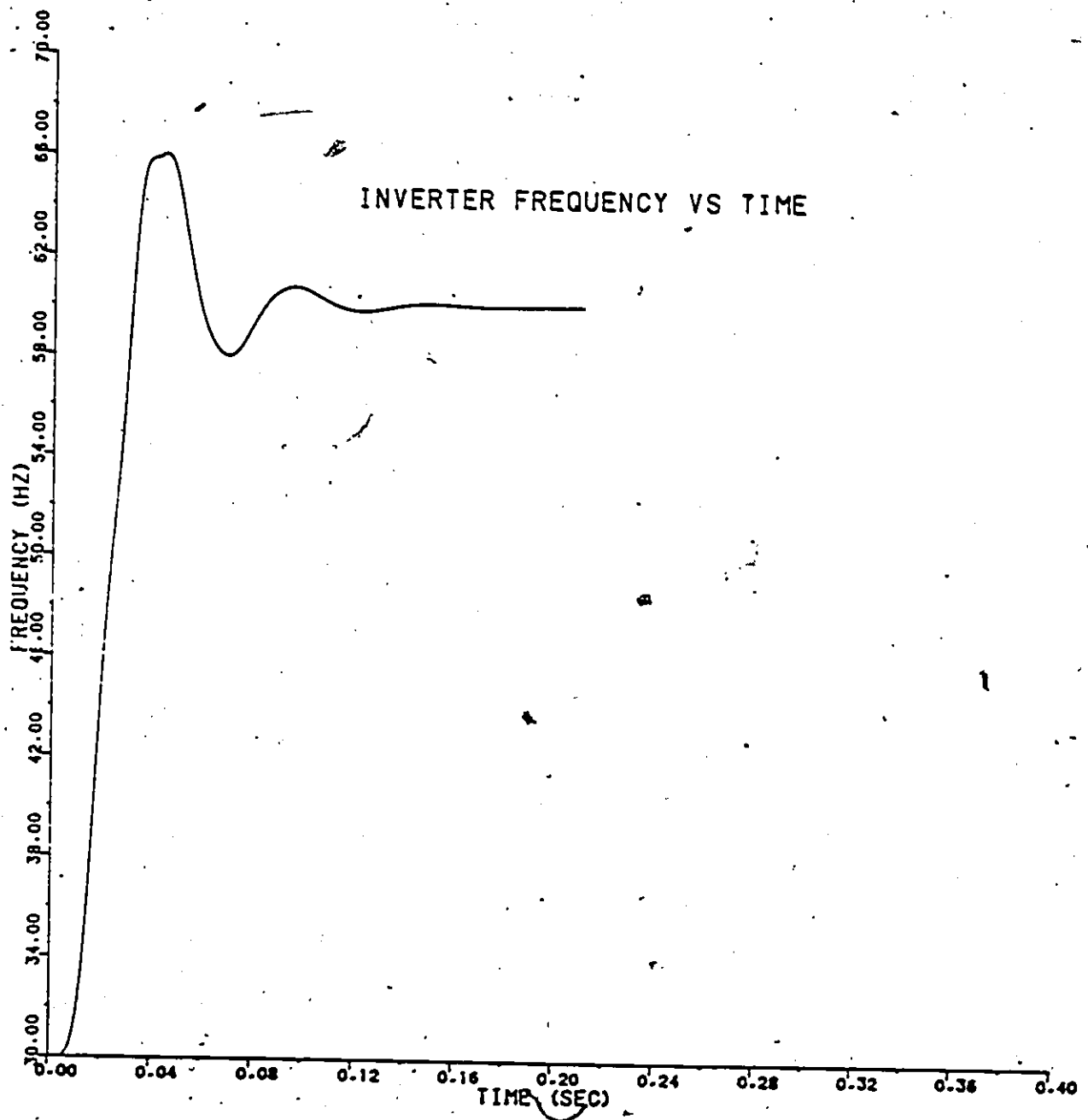


Figure 4.7 - Inverter Frequency-Time Curve during Starting

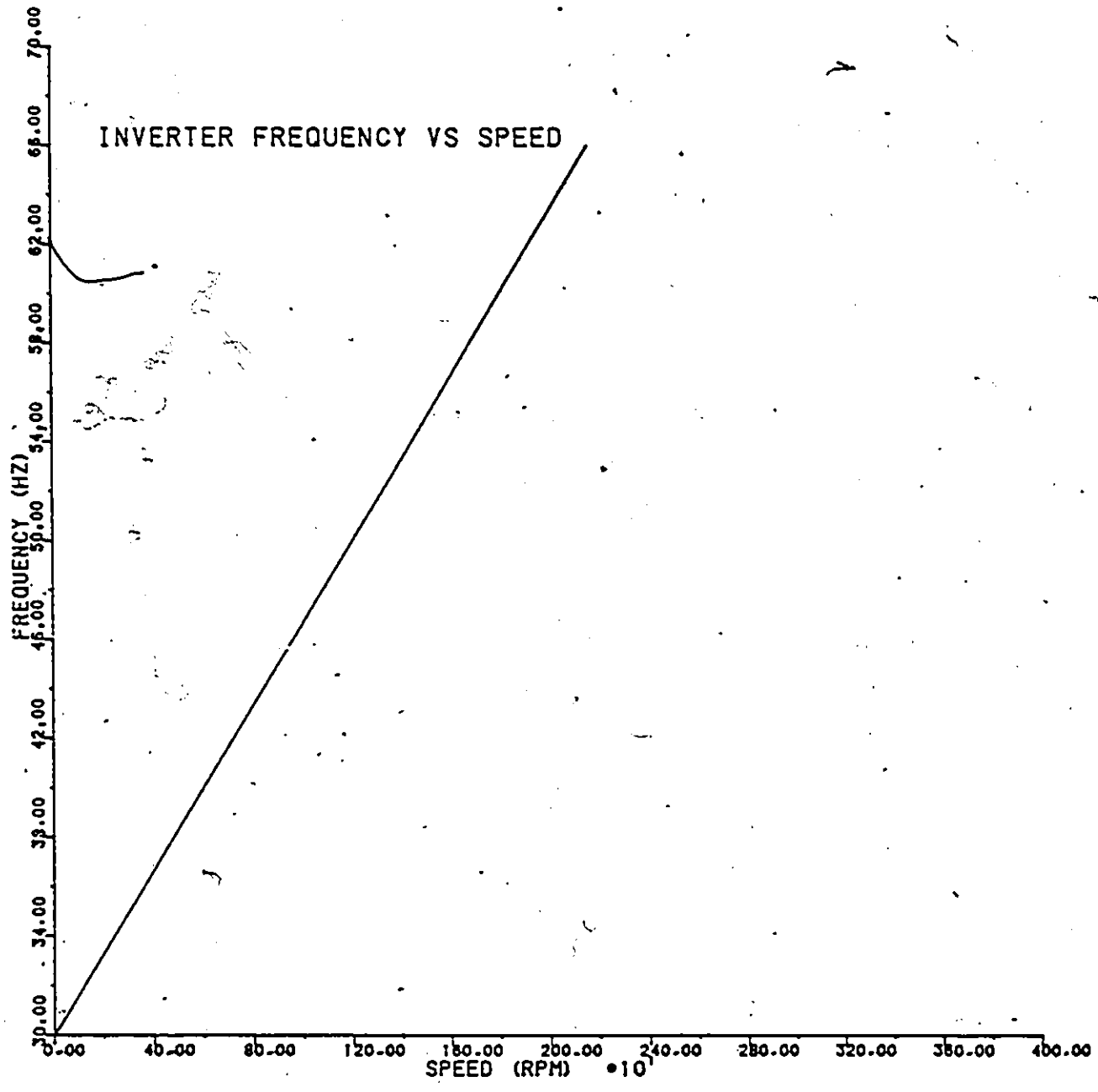
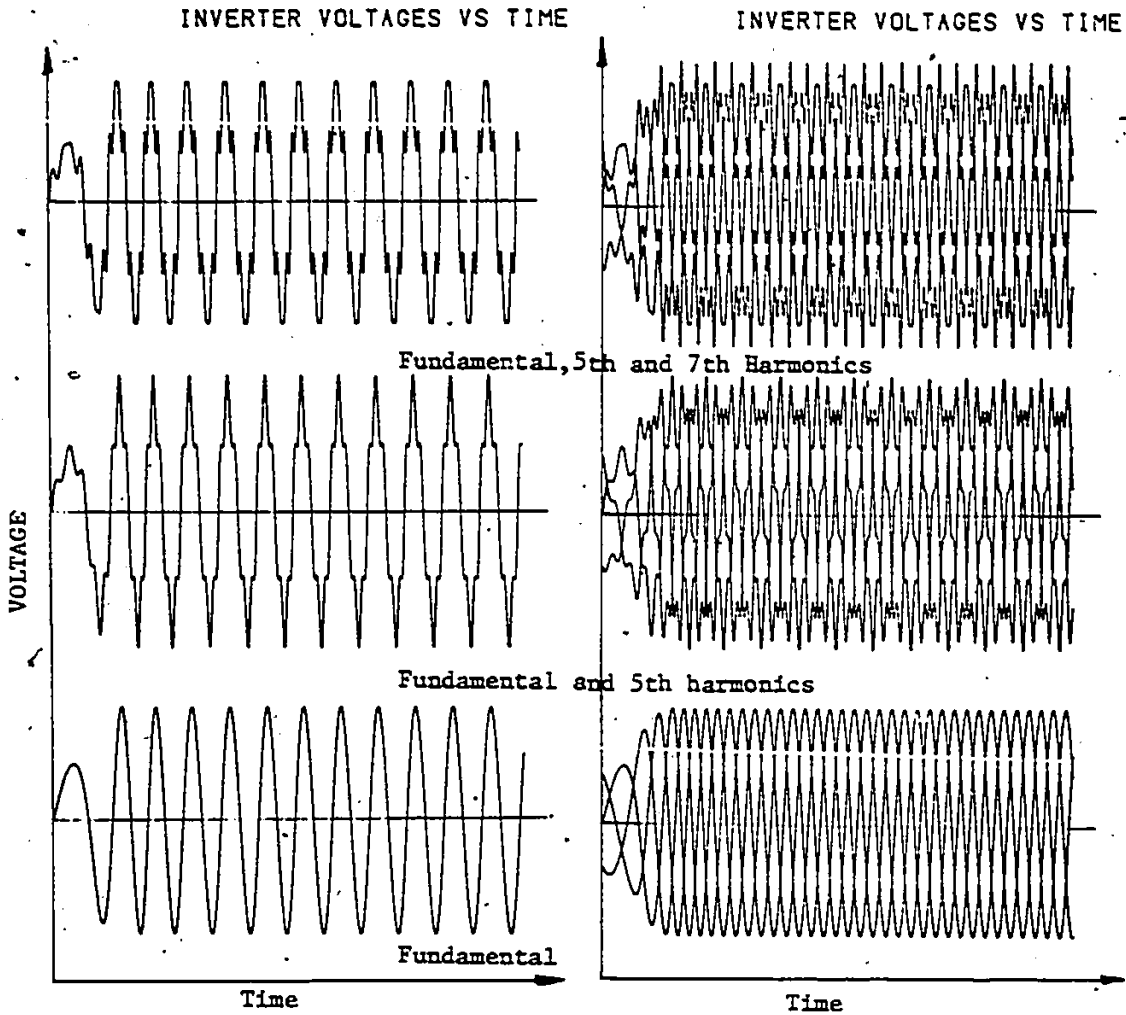


Figure 4.8 - Inverter Frequency-Speed Curve during Starting



(a)

(b)

Figure 4.9 - Computed Waveforms of Inverter output Voltages during Starting (a) Single Phase; (b) Three Phase

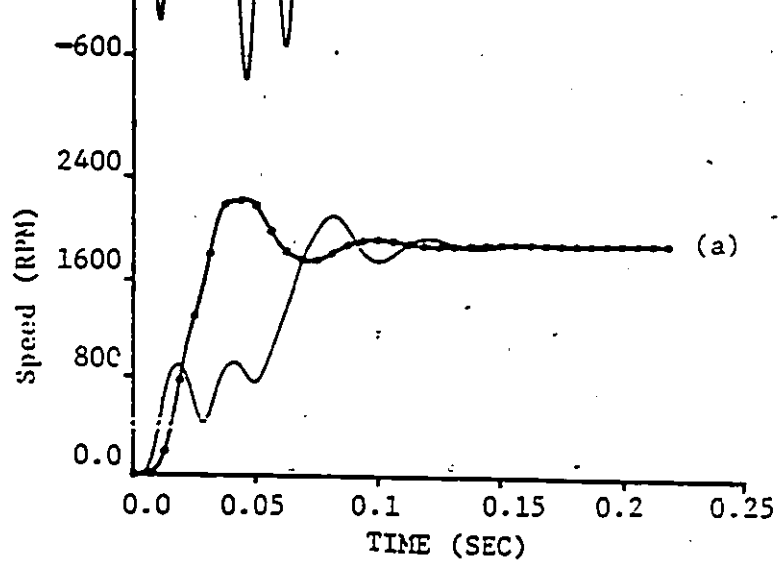
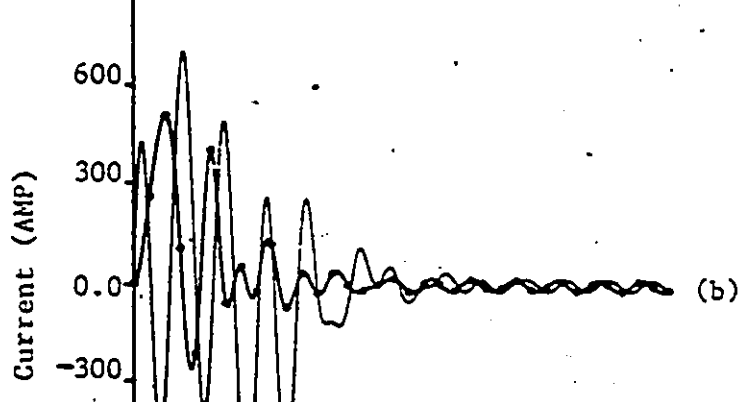
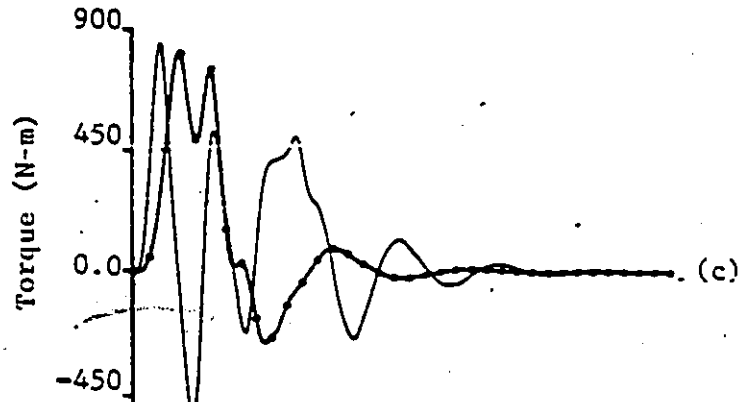
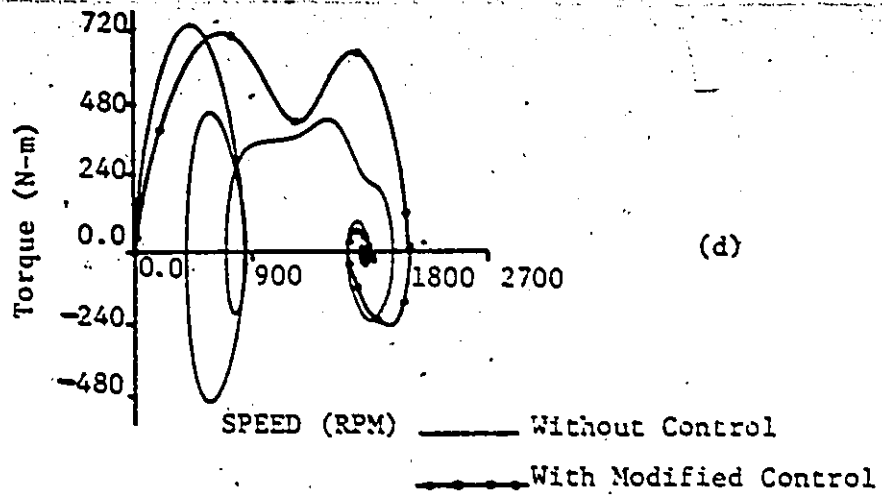


Figure 4.10 - Starting Transients with/without control (no-harmonics)

To see overall performance of the system at a glance Speed, Current and Torque characteristics are combined in Fig.4.10 & 4.15.

In the above method of simulation, there is an inversion of the time dependent matrix in every step of integration. To avoid this most inefficient computation operation, a second method is applied in which the voltage equations (3.2) of the induction motor were developed separately for the stator and rotor circuits. This method reduces the CPU time significantly, but introduces an error in the numerical results due to the presence of time-derivatives of state-variables on the right hand side of the equation (3.2). For comparison, the results obtained by the two methods are presented in Fig.4.10A. A complete listing of these programs have been given in Appendix A.

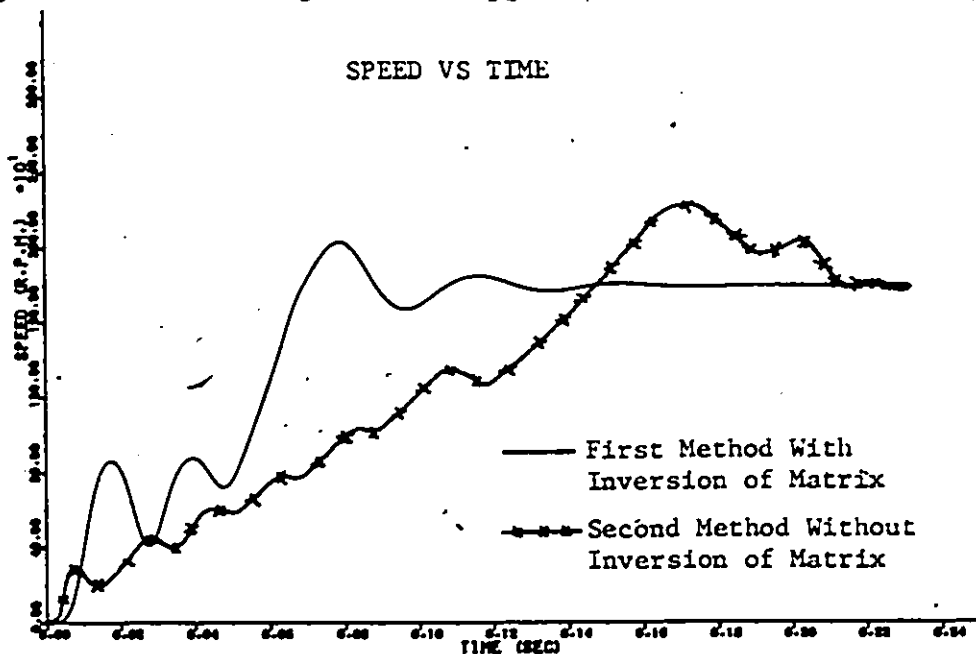


Fig.4.10A - Transient Build-up of Speed during Starting of The Motor

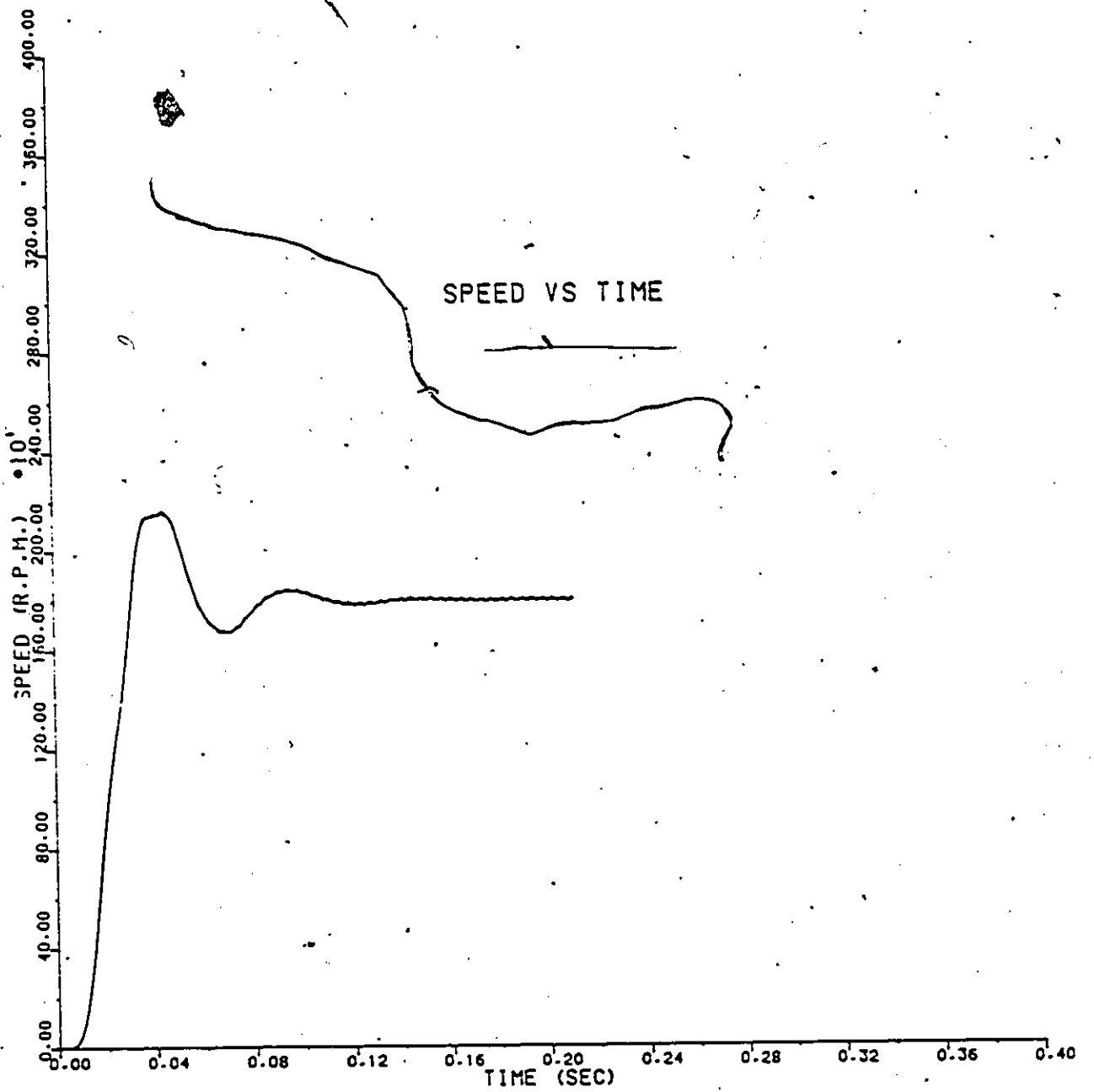


Figure 4.11 - Transient Speed Buildup during Starting with 5th and 7th harmonics

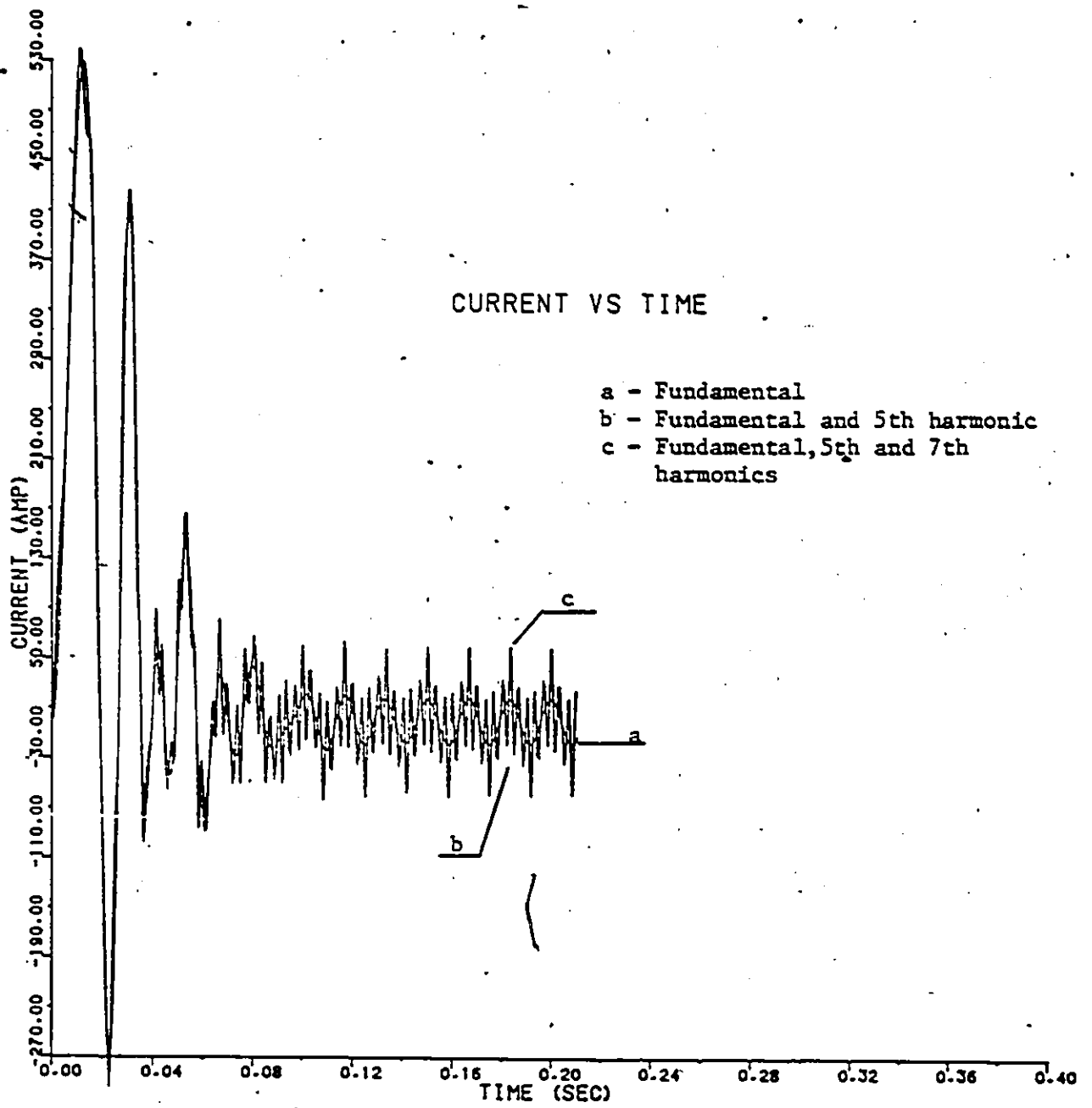


Figure 4.12 - Transient Current during starting with 5th and 7th harmonics

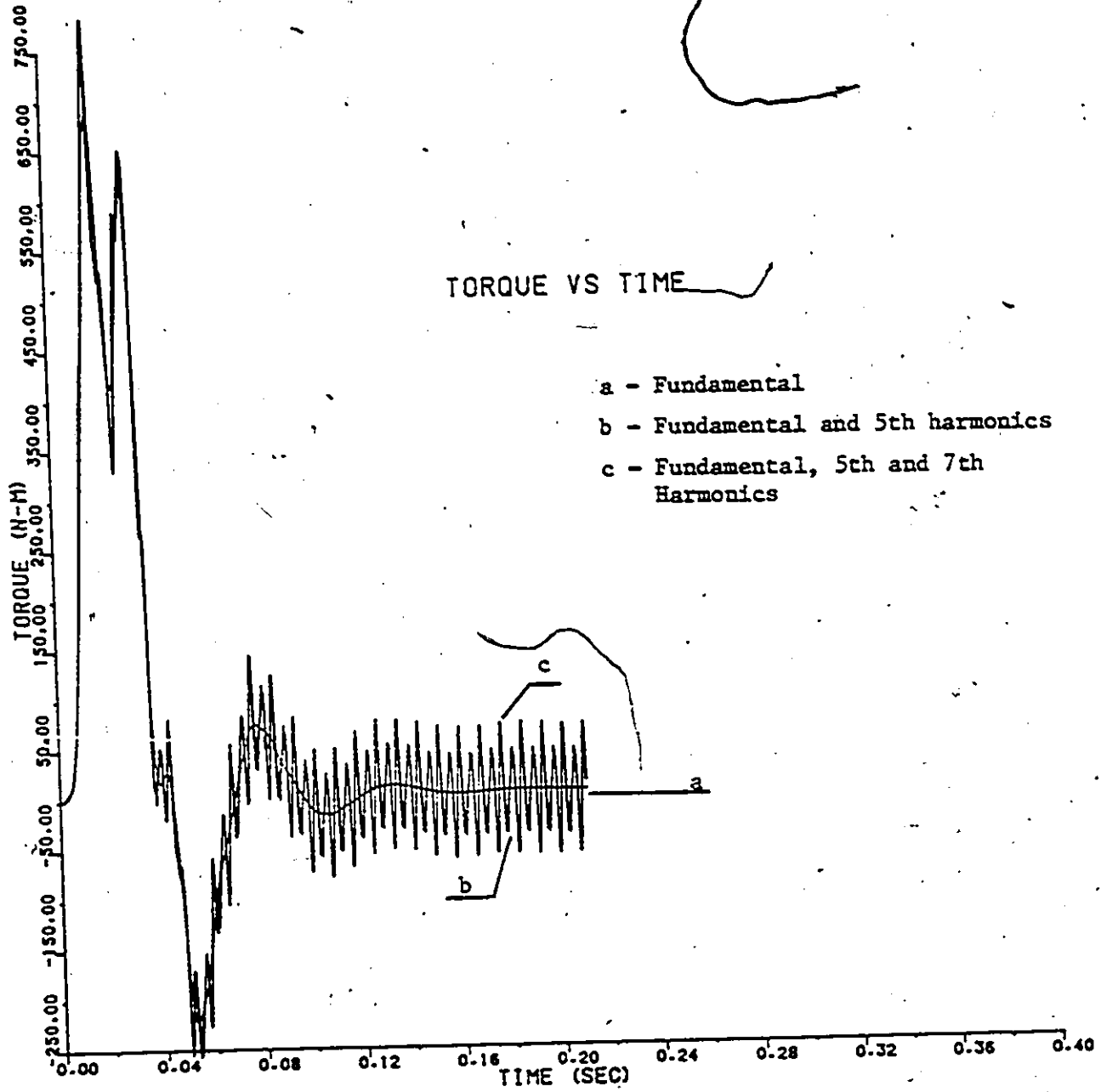


Figure 4.13 -- Transient Torque-Time Curves during Starting with 5th and 7th harmonics

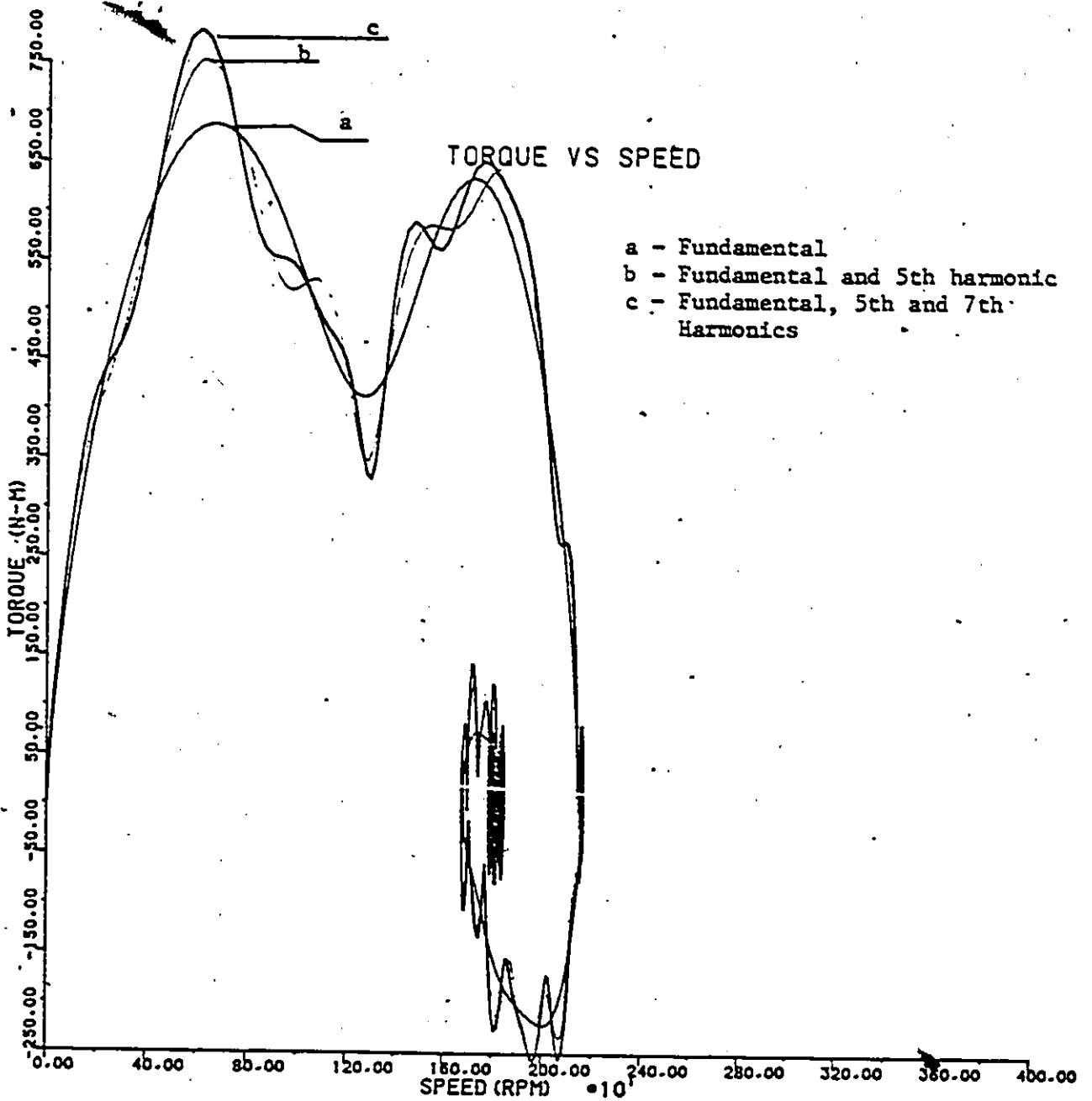


Figure 4.14 - Transient Torque-Speed Curves during Starting With 5th and 7th Harmonics

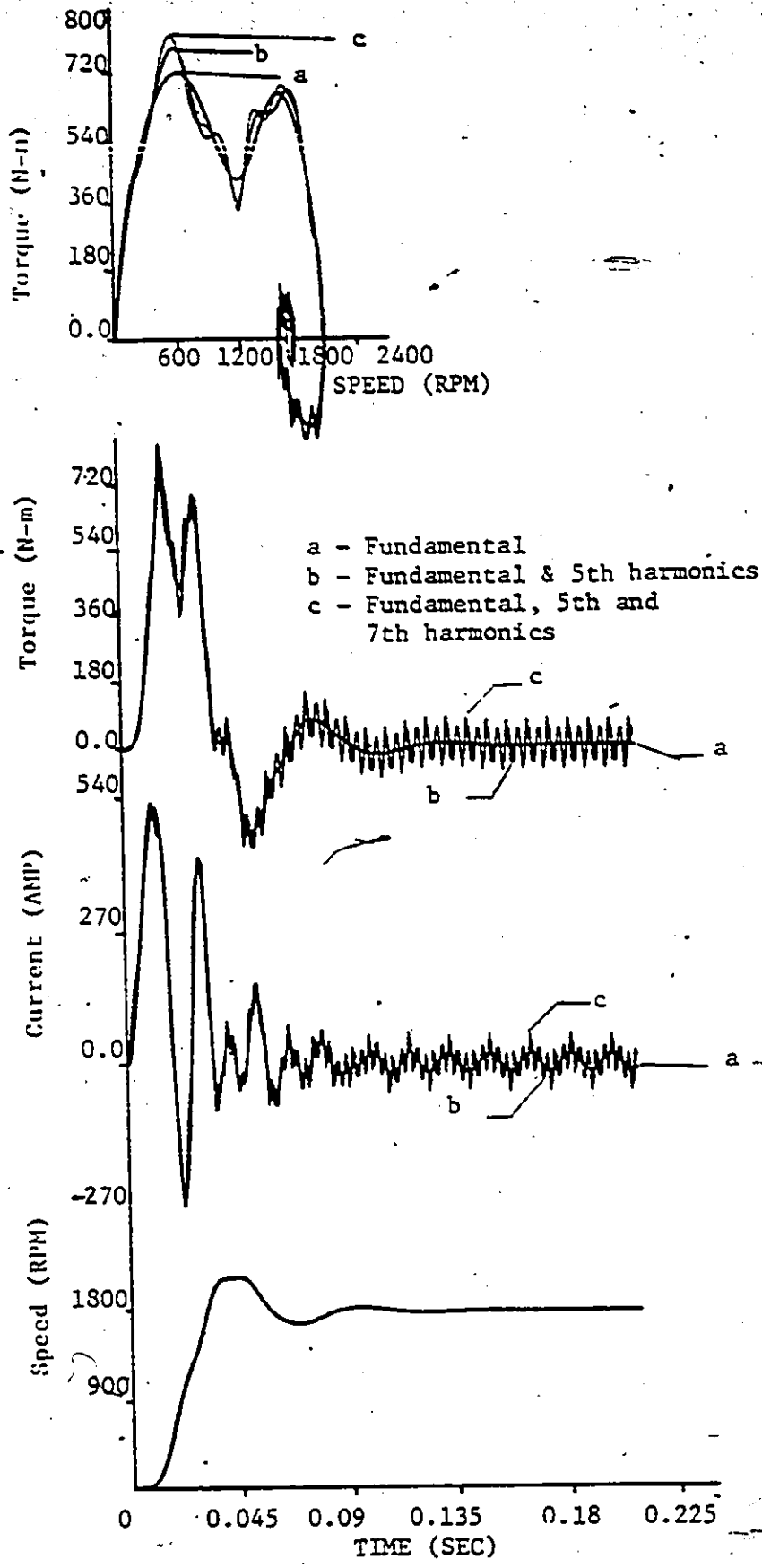


Figure 4.15 - Starting Transients with modified Control having 5th and 7th harmonics

4.2 NUMERICAL RESULTS

In order to verify the validity of the model developed and the digital simulation method employed, the following parameters were used.

Induction Motor Parameters:

The motor simulated in this study is a 4-pole, star connected squirrelcage induction motor with the following parameters:-

Magnetising Inductance (M) = 20.0 mH

Stator's self inductance (L_s) = 20.3925 mH

Rotor's self inductance referred to stator (L_r) = 20.3925 mH

Stator Resistance (r_1) = 0.063 Ohm

Rotor Resistance referred to stator (r_2) = 0.083 Ohm

Moment of Inertia (J) = 0.06 Kg-m

Friction Factor (K) = 0.03 Kg-m²/sec.

Horse Power = 30 H.P.

Terminal voltage (r.m.s) = 220V

Frequency = 60 Hz

Speed = 1789 rpm

Other System Parameters:

Phase detector constant (D_1) = 0.119 volt/rad

Voltage controlled oscillator constant (K_2) = 198.4164
rad/volt

Triggering Circuit constant (K_3) = 0.019 rad/volt

R_1 = 50,000 Ohms, R_2 = 5000 Ohms, C = 0.00005 μ F

ω_c = 2261.9467 rad

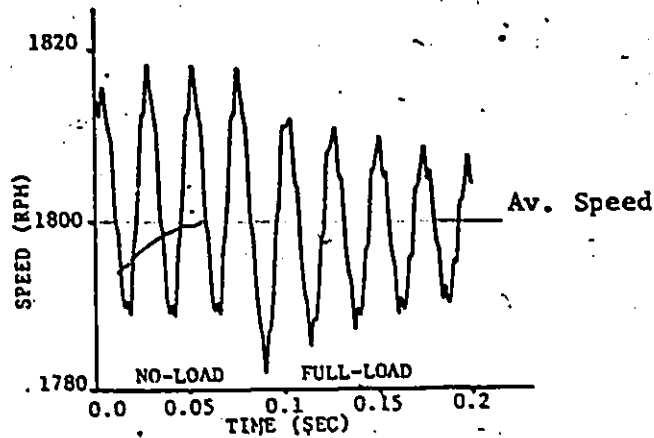


Figure 4.16 - No-Load;Full Load Response

The results of this analysis were compared with the reported results [1,5]. These results are matching favourably with the test results [1] and also with the computed results [5].

As shown in Fig.4.16, the overall motor speed is oscillatory due to low inertia of the system. From no-load/full load step response, the average speed before and after is almost same. The speed regulation is excellent of the order of $\pm 0.002\%$.

For better starting, the introduction of an inverter and time switch as indicated by block-S in Fig.1.2 substantially improves the starting performance of the system. This modification changes the frequency and the voltage of the VSI output to be proportional to the actual motor speed as shown in Fig.4.7-4.9. From Fig.4.2-4.5 one may observe the following facts:

(i) Fast and smooth starting : The run up time is reduced from 0.215sec to 0.135sec and oscillations are eliminated (Fig.4.2).

(ii) Low starting current : The starting current is reduced from 720 Amp(peak) to 520 Amp(peak) (Fig.4.3).

(iii) High starting torque : The starting torque remains almost constant throughout the starting period (550 N-m Av.) and high frequency oscillations are eliminated (Fig.4.4-5).

Further/ the time domain analysis also provides the overall effect of harmonics (5th,7th,11th,13th,.....) of the VSI output on the system behavior (as shown in Fig.4.11-4.14). The presence of the harmonics in the motor input voltage increases the undesired speed oscillations due to the pulsating torque components. However, there is no change in steady state torque of the system since the pulsating torque have zero average value.

CONCLUSION

In this thesis, for the analysis of a precise and adjustable speed AC drive system (Fig.1.2), a time domain model has been developed and simulated on a digital computer. The results and information obtained by this method, especially on starting behaviour of the system, are superior in comparison to the frequency domain method.

A modification (incorporation of an inverter and a time switch block-S) has been suggested for fast and smooth run up, high torque and low current peaks which are highly desirable for smooth and safe starting. This improves the starting performance significantly. The author feels that, in the applications requiring high starting torque (such as traction, crusher and grinders etc.), the squirrel-cage induction motor could be used in place of expensive slip-ring induction motor.

For efficient computation, for the analysis of AC drive system, usually d-q transformation is used under certain assumptions (e.g. balanced and symmetrical windings/power supplies, absence of any harmonics etc.). However, where these assumptions are not valid, as in this system due to

the presence of VSI harmonics, d-q transformation can not be applied. In this analysis to reduce the CPU time, as mentioned earlier, a second method for simulation has been tried, where the stator and rotor voltage equation (3.2) are developed separately to avoid the inversion of the matrix (L) in every step of the computation. This method introduces an error in the numerical results due to the presence of the time-derivatives of the state-variables on the right hand side of the system equations but it is insignificant for a qualitative analysis, such as the one presented here.

The time domain method used here is excellent and provides valuable information on dynamic and steady-state performance which is not possible by frequency domain method. It helps to study the system performance for different values of system parameters before implementation of the design. This method permits the study of the effect of harmonics as well as unbalanced/unsymmetrical systems such as single phase induction motor.

Scope of Further Research:

(i) The model developed and simulation method presented here could be easily modified for systems having current source inverter (CSI) in place of a voltage source inverter (VSI) and a synchronous motor in place of an induction motor.

(ii) The proposed control scheme (Fig.1.2) can be verified on an actual system in a laboratory.

(iii) This control scheme could be further improved by designing a time optimal controller which can be introduced between the filter and the phase-frequency detector blocks (Fig.1.2). This type of controls are required in multi-speed drive applications such as sugar mills, paper mills etc. for step change of speed.

(iv) For an efficient starting (i.e. fastest speed build-up, maximum starting torque and lowest current peaks), the model could be further modified by choosing a proper control function at the input stages of the VSI.

APPENDIX - A

Program No.1 - System without Harmonics

```

C THIS PROGRAM IS DOING THE ANALYSIS AND DIGITAL SIMULATION OF INDUCTION MOTOR
C 30 H.P.,220V(LINE),4-POLE,60 HZ,Y-CONNECTED WHICH IS COUPLED WITH THE LOAD
C OF TORQUE T=0.06 WM'+ 0.03 WM N-M,WHERE WM-MOTOR SPEED IN RADIAN/SEC
C THIS COMMON BLOCK DO INITIALISATION AND READ PARAMETERS OFTHE SYSTEM
C USED IN THE MAIN & SUBROUTINES
BLOCK DATA
REAL L(6,6),R(6,6),RJ,RK,V(8),INVL(6,6),DERL(6,6),IS
INTEGER P,NA
COMMON /MIT / L,R,P,RJ,RK,V,INVL,DERL,NA,TIME(703),
XTORQUE(703),VARF(703),SPEED(703),IS(703),PDERL(6,6)
DATA L(1,1),L(2,2),L(3,3),L(4,4),L(5,5),L(6,6),L(1,2),
X L(1,3),L(2,1),L(2,3),L(3,1),L(3,2),L(4,5),L(4,6),L(5,4),
X L(5,6),L(6,4),L(6,5),P,RJ,RK,R/6*20.3925,12*-10.0,4,0.06,
X 0.03,0.063,6*0.0,0.063,6*0.0,0.063,6*0.0,0.083,6*0.0,0.083,
X 6*0.0,0.083/
DATA V,PDERL,NA/8*0.0,36*0.0,0/
END
C THIS BLOCK USE CRKS SUBROUTINE TO SOLVE THE SYSTEM EQUATIONS
REAL L,INVL,IS
INTEGER P,NA
DIMENSION Y(10),DERY(10),PRMT(5),A(8,8),B(8,8),AUX(4,10),
X L(6,6),R(6,6),V(8),INVL(6,6),DERL(6,6)
C
COMMON /MIT / L,R,P,RJ,RK,V,INVL,DERL,NA,TIME(703),
XTORQUE(703),VARF(703),SPEED(703),IS(703),PDERL(6,6)
EXTERNAL FCT,OUTP,CRKS,MATINV,MATPLY,CRKS1,FCT1
DO 3 I=1,8
Y(I)=0.0
DERY(I)=1./8.
3 CONTINUE
NDIM=8
PRMT(1)=0.0
PRMT(2)=0.21
PRMT(3)=0.0003
PRMT(4)=0.00001
PRMT(5)=0.0
CALL CRKS1 (PRMT,Y,DERY,NDIM,IHLF,FCT1,OUTP,AUX)
C NOW WRITE THE TIME,STATOR CURRENT,TORQUE,SPEED,VARF
WRITE(6,100) NA
100 FORMAT ( 2X,I5//)
WRITE (6,5)
5 FORMAT ('0',2X,'TIME',T24,'STATOR CURRENT',T44,'TORQUE',
X T62,'SPEED',T82,'VARF'//)
DO 10 I=1,NA
C WRITE (6,6) TIME(I),IS(I),TORQUE(I),SPEED(I),VARF(I)
6 FORMAT ('0',5(E15.7,5X))
10 CONTINUE
C THIS PROGRAM PLOTS SPEED VS TIME
C
C
C SELECT SIZE OF PAPER 30CM X 27.5CM
CALL PLOTS (30.0,27.5)
C
C CALL FACTOR (0.50)
C SET THE ORIGIN
CALL PLOT (7.5,7.5,-3)

```



```

C RUNGE KUTTA GILL CLASSICAL SUBROUTINE
SUBROUTINE CRKS(PRMT,Y,DERY,NDIM,IHLF,FCT,OUTP,AUX)
DIMENSION Y(10),DERY(10),PRMT(5),AUX(4,10),YY(10)
X=PRMT(1)
XEND=PRMT(2)
H=PRMT(3)
IHLF=0
1 IF(X-XEND) 2,2,9
2 CALL FCT(X,Y,DERY)
CALL OUTP(X,Y,DERY,IHLF,NDIM,PRMT)
DO 7 K=1,4
DO 6 I=1,NDIM
GO TO (3,4,4,5),K
3 YY(I)=Y(I)
GO TO 6
4 YY(I)=Y(I)+AUX(K-1,I)*0.5
GO TO 6
5 YY(I)=Y(I)+AUX(K-1,I)
6 CONTINUE
CALL FCT(X,YY,DERY)
DO 7 I=1,NDIM
7 AUX(K,I)=H*DERY(I)
DO 8 I=1,NDIM
DY=(AUX(1,I)+2.0*AUX(2,I)+2.0*AUX(3,I)+AUX(4,I))/6.0
8 Y(I)=Y(I)+DY
X=X+H
GO TO 1
9 RETURN
END

```

C THIS PROGRAM DEVELOP SUBROUTINE FCT- FOR THE EQUATIONS TO BE SOLVED
C

```

SUBROUTINE FCT (X,Y,DERY)
REAL L,INVL,IS
INTEGER P,NA
COMMON /MIT/L,R,P,RJ,RK,V,INVL,DERL,NA,TIME,TORQUE,VARF,SPEED,
X IS,PDERL
DIMENSION Y(10),DERY(10),H(6,12),SUM(6,6),FUN(6,6),BY(8),AY(8),
XPDERL(6,6),TI(1,6),FUNI(1,6),A(8,8),B(8,8),V(8),L(6,6),DERL(6,6),
XR(6,6),TIME(703),IS(703),INVL(6,6),TORQUE(703),VARF(703),
XSPEED(703),LA(6),MA(6),S(6,6)
PIA=22./7.
ALPHA=0.1900*Y(9)
IF (DERY(10).GT.377.) ALPHA=0.0
VCO=3.*SQRT(2.)*160.*COS(ALPHA)/PIA
V(1)=3.*VCO*SIN(Y(10))/PIA
V(2)=3.*VCO*SIN(Y(10)-2.*PIA/3.)/PIA
V(3)=3.*VCO*SIN(Y(10)+2.*PIA/3.)/PIA
THETA=Y(8)
L(1,4)=20.*COS(THETA)
L(2,5)=L(1,4)
L(3,6)=L(1,4)
L(4,1)=L(1,4)
L(5,2)=L(1,4)
L(6,3)=L(1,4)
L(1,5)=20.*COS(THETA+2.*PIA/3.)

```

Cont.

```

L(2,6)=L(1,5)
L(3,4)=L(1,5)
L(4,3)=L(1,5)
L(5,1)=L(1,5)
L(6,2)=L(1,5)
L(1,6)=20.*COS(THETA-2.*PIA/3.)
L(2,4)=L(1,6)
L(3,5)=L(1,6)
L(4,2)=L(1,6)
L(5,3)=L(1,6)
L(6,1)=L(1,6)
PDERL(1,4)=-20.*SIN(THETA)
PDERL(2,5)=PDERL(1,4)
PDERL(3,6)=PDERL(1,4)
PDERL(4,1)=PDERL(1,4)
PDERL(5,2)=PDERL(1,4)
PDERL(6,3)=PDERL(1,4)
PDERL(1,5)=-20.*SIN(THETA+2.*PIA/3.)
PDERL(2,6)=PDERL(1,5)
PDERL(3,4)=PDERL(1,5)
PDERL(4,3)=PDERL(1,5)
PDERL(5,1)=PDERL(1,5)
PDERL(6,2)=PDERL(1,5)
PDERL(1,6)=-20.*SIN(THETA-2.*PIA/3.)
PDERL(2,4)=PDERL(1,6)
PDERL(3,5)=PDERL(1,6)
PDERL(4,2)=PDERL(1,6)
PDERL(5,3)=PDERL(1,6)
PDERL(6,1)=PDERL(1,6)
DO 3 I=1,6
DO 3 J=1,6
DERL(I,J)=PDERL(I,J)*DERY(8)
3 CONTINUE
K=6
M=12
CALL MATINV(INVL,L,K,M,H)
DO 1 I=1,6
DO 1 J=1,6
SUM(I,J)=R(I,J)+DERL(I,J)*.001
1 CONTINUE
CALL MATPLY(FUN,INVL,SUM,K,K,K)
DO 2 I=1,6
DO 2 J=1,6
A(I,J)=-FUN(I,J)*1000.
2 CONTINUE
DO 4 K=1,6
TI(1,K)=Y(K)
4 CONTINUE
N=1
M=6
K=6
CALL MATPLY(FUNI,TI,PDERL,N,M,K)
DO 5 I=1,6
A(7,I)=(1./RJ)*FUNI(1,I)*.001
5 CONTINUE

```

Cont. . .

```

DO 6 J=7,8
DO 6 I=1,6
A(I,J)=0.0
6 CONTINUE
DO 7 I=1,6
A(8,I)=0.0
7 CONTINUE
A(7,7)=-RK/RJ
A(7,8)=0.0
A(8,7)=P/2.
A(8,8)=0.0
C DEVELOP THE MATRIX B
C

```

```

DO 8 I=1,6
DO 8 J=1,6.
B(I,J)=INVL(I,J)*1000.
8 CONTINUE
DO 9 J=7,8
DO 9 I=1,8
B(I,J)=0.0
9 CONTINUE
DO 10 I=7,8
DO 10 J=1,6
B(I,J)=0.0
10 CONTINUE
N=8
M=8
K=1
CALL MATPLY(BV,B,V,N,M,K)
CALL MATPLY(AY,A,Y,N,M,K)
DO 11 I=1,8
DERY(I)=AY(I)+BV(I)
11 CONTINUE
DERY(9)=-0.0133*DERY(7)*5.7/2.5
DERY(10)=2261.9467/6.-198.4164*Y(9)/6.
RETURN
END

```

CTHIS SUBROUTINE OUTP WILL CALCULATRE THE OUTPUTPARAMETERS OF THE SYSTEM
CSUCH AS TORQUE,SPEED,VARF

```

SUBROUTINE OUTP(X,Y,DERY,IHLF,NDIM,PRMT)
REAL L,INVL,IS
INTEGER P,NA
COMMON /MIT/L,R,P,RJ,RK,V,INVL,DERL,NA,TIME,TORQUE,VARF,SPEED,
XIS,PDERL
DIMENSION Y(10),DERY(10),CUR(6),PDERL(6,6),TI(1,6),PDERLI(6),
XTORQUE(703),SPEED(703),VARF(703),L(6,6),R(6,6),V(8),
XINVL(6,6),DERL(6,6),TIME(703),IS(703),PRMT(5)
PIA=22./7.
DO 1 K=1,6
CUR(K)=Y(K)
1 CONTINUE
N=6
K=1
CALL MATPLY(PDERLI,PDERL,CUR,N,N,K)

```

```

DO 2 J=1,6
2   TI(1,J)=CUR(J)
   N=1
   M=6
   K=1
   CALL MATPLY(TDERLI, TI, PDERLI, N, M, K)
   NA=NA+1
   TIME(NA)=X
   IS(NA)=Y(1)
   TORQUE(NA)=TDERLI*.001
   OMGM=Y(7)
   SPEED(NA)=OMGM*60./(2.*PIA)
C   OPTICAL ENCODER OUTPUT FOR THE DISC OF 36 HOLES MOUNTED ON THE SHAFT
   VARF(NA)=OMGM*36/(2.*PIA)
C   WRITE (6,6) V(1),V(2),V(3),Y(7),Y(9),Y(10),DERY(10)
6   FORMAT ('0',7(E15.7,2X))
   5   CONTINUE
   RETURN
   END

```

CTHIS SUBROUTINE DO THE INVERSION OF MATRIX A(N,N) BY USING AUXILIARY
C MATRIX H(N,2*N) AND AUGUMENTING THE MATRIX A WITH THE UNIT MATRIX OF
C SAME DIMENSION (N,N)

```

SUBROUTINE MATINV(INVA, A, N, N2, H)
REAL INVA
DIMENSION A(6,6), INVA(6,6), H(6,12)
DO 1 I=1, N
DO 1 J=1, N
1   H(I,J)=A(I,J)
   N1=N+1
DO 2 I=1, N
DO 3 J=N1, N2
   N3=I+N
   IF (N3-J) 4,5,4
5   H(I,J)=1.0
   GO TO 3
4   H(I,J)=0.0
3   CONTINUE
2   CONTINUE
DO 6 I=1, N
   D=H(I,I)
DO 7 J=1, N2
7   H(I,J)=H(I,J)/D
DO 8 L=1, N
   IF (L.EQ.I) GO TO 8
   E=H(L,I)
DO 9 J=1, N2
9   H(L,J)=H(L,J)-E*H(I,J)
8   CONTINUE
6   CONTINUE
DO 10 I=1, N
DO 10 J=N1, N2
10  -INVA(I, J-N)=H(I,J)
   RETURN
   END

```

C
C
C
C
C

THIS SUBROUTINE MATPLY DO THE MULTIPLICATION OF TWO MATRIX
A(N,M) AND B(M,L)

```
3 SUBROUTINE MATPLY(AB,A,B,N,M,L)
2 DIMENSION AB(N,L),A(N,M),B(M,L)
1 DO 1 K=1,N
  DO 2 I=1,L
    SUM=0.0
    DO 3 J=1,M
      SUM=SUM+A(K,J)*B(J,I)
    CONTINUE
  AB(K,I)=SUM
  CONTINUE
CONTINUE
RETURN
END
```

C

RUNGE KUTTA GILL CLASSICAL SUBROUTINE
SUBROUTINE CRKS1(PRMT,Y,DERY,NDIM,IHLF,FCT1,OUTP,AUX)
DIMENSION Y(10),DERY(10),PRMT(5),AUX(4,10),YY(10)
X=PRMT(1)
XEND=PRMT(2)
H=PRMT(3)
IHLF=0

1
2
3
4
5
6
7
8
9

```
  IF(X-XEND) 2,2,9
  CALL FCT1(X,Y,DERY)
  CALL OUTP(X,Y,DERY,IHLF,NDIM,PRMT)
  DO 7 K=1,4
    DO 6 I=1,NDIM
      GO TO (3,4,4,5),K
  YY(I)=Y(I)
  GO TO 6
  YY(I)=Y(I)+AUX(K-1,I)*0.5
  GO TO 6
  YY(I)=Y(I)+AUX(K-1,I)
  CONTINUE
  CALL FCT1(X,YY,DERY)
  DO 7 I=1,NDIM
    AUX(K,I)=H*DERY(I)
  DO 8 I=1,NDIM
    DY=(AUX(1,I)+2.0*AUX(2,I)+2.0*AUX(3,I)+AUX(4,I))/6.0
  Y(I)=Y(I)+DY
  X=X+H
  GO TO 1
RETURN
END
```

C
C

THIS PROGRAM DEVELOP SUBROUTINE FCT- FOR THE EQUATIONS TO BE SOLVED

```
  SUBROUTINE FCT1 (X,Y,DERY)
  REAL L,INVL,IS
  INTEGER P,NA
  COMMON /MIT/L,R,P,RJ,RK,V,INVL,DERL,NA,TIME,TORQUE,VARF,SPEED,
  X IS,PDERL
```

```
DIMENSION Y(10),DERY(10),H(6,12),SUM(6,6),FUN(6,6),BV(8),AY(8),
XPDERL(6,6),TI(1,6),FUNI(1,6),A(8,8),B(8,8),V(8),L(6,6),DERL(6,6),
XR(6,6),TIME(703),IS(703),INVL(6,6),TORQUE(703),VARF(703),
XSPEED(703),LA(6),MA(6),S(6,6)
```

```
PIA=22./7.
```

```
V(1)=180.*COS(377.*X)
```

```
V(2)=180.*COS(377.*X-2.*PIA/3.)
```

```
V(3)=180.*COS(377.*X+2.*PIA/3.)
```

```
THETA=Y(8)
```

```
L(1,4)=20.*COS(THETA)
```

```
L(2,5)=L(1,4)
```

```
L(3,6)=L(1,4)
```

```
L(4,1)=L(1,4)
```

```
L(5,2)=L(1,4)
```

```
L(6,3)=L(1,4)
```

```
L(1,5)=20.*COS(THETA+2.*PIA/3.)
```

```
L(2,6)=L(1,5)
```

```
L(3,4)=L(1,5)
```

```
L(4,3)=L(1,5)
```

```
L(5,1)=L(1,5)
```

```
L(6,2)=L(1,5)
```

```
L(1,6)=20.*COS(THETA-2.*PIA/3.)
```

```
L(2,4)=L(1,6)
```

```
L(3,5)=L(1,6)
```

```
L(4,2)=L(1,6)
```

```
L(5,3)=L(1,6)
```

```
L(6,1)=L(1,6)
```

```
PDERL(1,4)=-20.*SIN(THETA)
```

```
PDERL(2,5)=PDERL(1,4)
```

```
PDERL(3,6)=PDERL(1,4)
```

```
PDERL(4,1)=PDERL(1,4)
```

```
PDERL(5,2)=PDERL(1,4)
```

```
PDERL(6,3)=PDERL(1,4)
```

```
PDERL(1,5)=-20.*SIN(THETA+2.*PIA/3.)
```

```
PDERL(2,6)=PDERL(1,5)
```

```
PDERL(3,4)=PDERL(1,5)
```

```
PDERL(4,3)=PDERL(1,5)
```

```
PDERL(5,1)=PDERL(1,5)
```

```
PDERL(6,2)=PDERL(1,5)
```

```
PDERL(1,6)=-20.*SIN(THETA-2.*PIA/3.)
```

```
PDERL(2,4)=PDERL(1,6)
```

```
PDERL(3,5)=PDERL(1,6)
```

```
PDERL(4,2)=PDERL(1,6)
```

```
PDERL(5,3)=PDERL(1,6)
```

```
PDERL(6,1)=PDERL(1,6)
```

```
DO 3 I=1,6
```

```
DO 3 J=1,6
```

```
DERL(I,J)=PDERL(I,J)*DERY(8)
```

```
CONTINUE-
```

```
K=6
```

```
M=12
```

```
CALL MATINV(INVL,L,K,M,H)
```

```
DO 1 I=1,6
```

```
DO 1 J=1,6
```

```
SUM(I,J)=R(I,J)+DERL(I,J)*.001
```

```
CONTINUE
```

Cont.

```

CALL MATPLY(FUN,INVL,SUM,K,K,K)
DO 2 I=1,6
DO 2 J=1,6
A(I,J)=-FUN(I,J)*1000.
2 CONTINUE
DO 4 K=1,6
TI(1,K)=Y(K)
4 CONTINUE
N=1
M=6
K=6
CALL MATPLY(FUNI,TI,PDERL,N,M,K)
DO 5 I=1,6
A(7,I)=(1.0/RJ)*FUNI(1,I)*.001
5 CONTINUE
DO 6 J=7,8
DO 6 I=1,6
A(I,J)=0.0
6 CONTINUE
DO 7 I=1,6
A(8,I)=0.0
7 CONTINUE
A(7,7)=-RK/RJ
A(7,8)=0.0
A(8,7)=P/2.
A(8,8)=0.0
C DEVELOP THE MATRIX B
C
DO 8 I=1,6
DO 8 J=1,6
B(I,J)=INVL(I,J)*1000.
8 CONTINUE
DO 9 J=7,8
DO 9 I=1,8
B(I,J)=0.0
9 CONTINUE
DO 10 I=7,8
DO 10 J=1,6
B(I,J)=0.0
10 CONTINUE
N=8
M=8
K=1
CALL MATPLY(BV,B,V,N,M,K)
CALL MATPLY(AY,A,Y,N,M,K)
DO 11 I=1,8
DERY(I)=AY(I)+BV(I)
11 CONTINUE
RETURN
END

```

Program No.2 - System with Harmonics

C THIS PROGRAM IS DOING THE ANALYSIS AND DIGITAL SIMULATION OF INDUCTION MOTOR
 C 30 H.P., 220V(LINE), 4-POLE, 60 HZ, Y-CONNECTED WHICH IS COUPLED WITH THE LOAD
 C OF TORQUE $T=0.06 \text{ WM}' + 0.03 \text{ WM N-M}$, WHERE WM-MOTOR SPEED IN RADIAN/SEC
 C THIS COMMON BLOCK DO INITIALISATION AND READ PARAMETERS OF THE SYSTEM
 C USED IN THE MAIN & SUBROUTINES.

BLOCK DATA

REAL L(6,6), R(6,6), RJ, RK, V(8), INVL(6,6), DERL(6,6), IS
 INTEGER P, NA
 COMMON /MIT / L, R, P, RJ, RK, V, INVL, DERL, NA, TIME(705),
 XTORQUE(705), VARF(705), SPEED(705), IS(705), PDERL(6,6), NR
 DATA L(1,1), L(2,2), L(3,3), L(4,4), L(5,5), L(6,6), L(1,2),
 X L(1,3), L(2,1), L(2,3), L(3,1), L(3,2), L(4,5), L(4,6), L(5,4),
 X L(5,6), L(6,4), L(6,5), P, RJ, RK, R/6*20.3925, 12*-10.0, 4, 0.06,
 X 0.03, 0.063, 6*0.0, 0.063, 6*0.0, 0.063, 6*0.0, 0.083, 6*0.0, 0.083,
 X 6*0.0, 0.083/
 DATA V, PDERL, NA, NR/8*0.0, 36*0.0, 0, 0/
 END

C THIS BLOCK USE CRKS SUBROUTINE TO SOLVE THE SYSTEM EQUATIONS

REAL L, INVL, IS
 INTEGER P, NA
 DIMENSION Y(10), DERY(10), PRMT(5), A(8,8), B(8,8), AUX(4,10),
 X L(6,6), R(6,6), V(8), INVL(6,6), DERL(6,6)

C
 COMMON /MIT / L, R, P, RJ, RK, V, INVL, DERL, NA, TIME(705),
 XTORQUE(705), VARF(705), SPEED(705), IS(705), PDERL(6,6), NR
 EXTERNAL FCT, OUTP, CRKS, MATINV, MATPLY

100 DO 4 I=1, 10
 Y(I)=0.0
 DERY(I)=1./10.
 4 CONTINUE
 Y(9)=5.7
 NDIM=10
 PRMT(1)=0.0
 PRMT(2)=0.21
 PRMT(3)=0.0003
 PRMT(4)=0.00001
 PRMT(5)=0.0
 IF (NR.EQ.1) GO TO 101
 IF (NR.EQ.2) GO TO 102

CALL CRKS (PRMT, Y, DERY, NDIM, IHLF, FCT, OUTP, AUX)

C NOW WRITE THE TIME, STATOR CURRENT, TORQUE, SPEED, VARF

C WRITE(6,100) NA
 C 100 FORMAT (2X, I5//)
 C WRITE (6,5)
 C 5 FORMAT ('0', 2X, 'TIME', T24, 'STATOR CURRENT', T44, 'TORQUE',
 C X T62, 'SPEED', T82, 'VARF'//)
 C DO 10 I=1, NA
 C WRITE (6,6) TIME(I), IS(I), TORQUE(I), SPEED(I), VARF(I).
 C 6 FORMAT ('0', 5(E15.7, 5X))

10 CONTINUE

Cont.


```

102 CALL CRKS (PRMT,Y,DERY,NDIM,IHLF,FCT,OUTP,AUX)
C USE GREEN PEN
  CALL NEWPEN (1)
    CALL LINE (TIME,SPEED,701,1,0,0)
    CALL PLOT (0.0,15.0,-3)
    CALL LINE (TIME,IS,701,1,0,0)
    CALL PLOT (0.0,18.0,-3)
    CALL LINE (TIME,TORQUE,701,1,0,0)
    CALL PLOT (0.0,21.0,-3)
    CALL LINE (SPEED,TORQUE,701,1,0,0)
  STOP PLOTTING
  CALL PLOT (0.0,0.0,999)
C
  STOP
  END
C RUNGE KUTTA GILL CLASSICAL SUBROUTINE
  SUBROUTINE CRKS (PRMT,Y,DERY,NDIM,IHLF,FCT,OUTP,AUX)
  DIMENSION Y(10),DERY(10),PRMT(5),AUX(4,10),YY(10)
  X=PRMT(1)
  XEND=PRMT(2)
  H=PRMT(3)
  IHLF=0
1 IF(X-XEND) 2,2,9
2 CALL FCT(X,Y,DERY)
  CALL OUTP(X,Y,DERY,IHLF,NDIM,PRMT)
  DO 7 K=1,4
  DO 6 I=1,NDIM
  GO TO (3,4,4,5),K
3 YY(I)=Y(I)
  GO TO 6
4 YY(I)=Y(I)+AUX(K-1,I)*0.5
  GO TO 6-
5 YY(I)=Y(I)+AUX(K-1,I)
6 CONTINUE
  CALL FCT(X,YY,DERY)
  DO 7 I=1,NDIM
7 AUX(K,I)=H*DERY(I)
  DO 8 I=1,NDIM
8 DY=(AUX(1,I)+2.0*AUX(2,I)+2.0*AUX(3,I)+AUX(4,I))/6.0
  Y(I)=Y(I)+DY
  X=X+H
  GO TO 1
9 RETURN
  END
C THIS PROGRAM DEVELOP SUBROUTINE FCT- FOR THE EQUATIONS TO BE SOLVED
C
  SUBROUTINE FCT (X,Y,DERY)
  REAL L,INVL,IS
  INTEGER P,NA
  COMMON /MIT/L,P,R,RJ,RK,V,INVL,DERL,NA,TIME,TORQUE,VARF,SPEED,
  X IS,PDERL,NR
  DIMENSION Y(10),DERY(10),H(6,12),SUM(6,6),FUN(6,6),BV(8),AY(8),
  XPDERL(6,6),TI(1,6),FUNI(1,6),A(8,8),B(8,8),V(8),L(6,6),DERL(6,6),
  XR(6,6),TIME(705),IS(705),INVL(6,6),TORQUE(705),VARF(705),
  XSPEED(705),LA(6),MA(6),S(6,6)

```

```

PIA=22./7.
ALPHA=0.1900*Y(9)
IF (DERY(10).GT.377.) ALPHA=0.0
VCO=3.*SQRT(2.)*160.*COS(ALPHA)/PIA
IF (NR.EQ.1) GO TO 100
IF (NR.EQ.2) GO TO 101
V(1)=3.*VCO*SIN(Y(10))/PIA
V(2)=3.*VCO*SIN(Y(10)-2.*PIA/3.)/PIA
V(3)=3.*VCO*SIN(Y(10)+2.*PIA/3.)/PIA
GO TO 102
100 V(1)=3.*VCO*(SIN(Y(10))+SIN(5.*Y(10))/5.)/PIA
V(2)=3.*VCO*(SIN(Y(10)-2.*PIA/3.)+SIN(5.*Y(10)-2.*PIA/3.)/5.)/PIA
V(3)=3.*VCO*(SIN(Y(10)+2.*PIA/3.)+SIN(5.*Y(10)+2.*PIA/3.)/5.)/PIA
GO TO 102
101 V(1)=3.*VCO*(SIN(Y(10))+SIN(5.*Y(10))/5.+SIN(7.*Y(10))/7.)/PIA
V(2)=3.*VCO*(SIN(Y(10)-2.*PIA/3.)+SIN(5.*Y(10)-2.*PIA/3.)/5.
X +SIN(7.*Y(10)-2.*PIA/3.)/7.)/PIA
V(3)=3.*VCO*(SIN(Y(10)+2.*PIA/3.)+SIN(5.*Y(10)+2.*PIA/3.)/5.
X +SIN(7.*Y(10)+2.*PIA/3.)/7.)/PIA
102 THETA=Y(8)
L(1,4)=20.*COS(THETA)
L(2,5)=L(1,4)
L(3,6)=L(1,4)
L(4,1)=L(1,4)
L(5,2)=L(1,4)
L(6,3)=L(1,4)
L(1,5)=20.*COS(THETA+2.*PIA/3.)
L(2,6)=L(1,5)
L(3,4)=L(1,5)
L(4,3)=L(1,5)
L(5,1)=L(1,5)
L(6,2)=L(1,5)
L(1,6)=20.*COS(THETA-2.*PIA/3.)
L(2,4)=L(1,6)
L(3,5)=L(1,6)
L(4,2)=L(1,6)
L(5,3)=L(1,6)
L(6,1)=L(1,6)
PDERL(1,4)=-20.*SIN(THETA)
PDERL(2,5)=PDERL(1,4)
PDERL(3,6)=PDERL(1,4)
PDERL(4,1)=PDERL(1,4)
PDERL(5,2)=PDERL(1,4)
PDERL(6,3)=PDERL(1,4)
PDERL(1,5)=-20.*SIN(THETA+2.*PIA/3.)
PDERL(2,6)=PDERL(1,5)
PDERL(3,4)=PDERL(1,5)
PDERL(4,3)=PDERL(1,5)
PDERL(5,1)=PDERL(1,5)
PDERL(6,2)=PDERL(1,5)
PDERL(1,6)=-20.*SIN(THETA-2.*PIA/3.)
PDERL(2,4)=PDERL(1,6)
PDERL(3,5)=PDERL(1,6)
PDERL(4,2)=PDERL(1,6)
PDERL(5,3)=PDERL(1,6)
PDERL(6,1)=PDERL(1,6)

```

Cont.

```

DO 3 I=1,6
DO 3 J=1,6
DERL(I,J)=PDERL(I,J)*DERY(8)
3 CONTINUE
K=6
M=12
CALL MATINV(INVL,L,K,M,H)
DO 1 I=1,6
DO 1 J=1,6
SUM(I,J)=R(I,J)+DERL(I,J)*.001
1 CONTINUE
CALL MATPLY(FUN,INVL,SUM,K,K,K)
DO 2 I=1,6
DO 2 J=1,6
A(I,J)=-FUN(I,J)*1000.
2 CONTINUE
DO 4 K=1,6
TI(1,K)=Y(K)
4 CONTINUE
N=1
M=6
K=6
CALL MATPLY(FUNI,TI,PDERL,N,M,K)
DO 5 I=1,6
A(7,I)=(1./RJ)*FUNI(1,I)*.001
5 CONTINUE
DO 6 J=7,8
DO 6 I=1,6
A(I,J)=0.0
6 CONTINUE
DO 7 I=1,6
A(8,I)=0.0
7 CONTINUE
A(7,7)=-RK/RJ
A(7,8)=0.0
A(8,7)=P/2.
A(8,8)=0.0
C DEVELOP THE MATRIX B
C
DO 8 I=1,6
DO 8 J=1,6
B(I,J)=INVL(I,J)*1000.
8 CONTINUE
DO 9 J=7,8
DO 9 I=1,8
B(I,J)=0.0
9 CONTINUE
DO 10 I=7,8
DO 10 J=1,6
B(I,J)=0.0
10 CONTINUE

```

Cont.

```

N=8
M=8
K=1
CALL MATPLY(BV,B,V,N,M,K)
CALL MATPLY(AY,A,Y,N,M,K)
DO 11 I=1,8
  DERY(I)=AY(I)+BV(I)
11 CONTINUE
  DERY(9)=-0.0133*DERY(7)*5.7/2.5
  DERY(10)=2261.9467/6.-198.4164*Y(9)/6.
  RETURN
  END

```

CTHIS SUBROUTINE OUTP WILL CALCULATRE THE OUTPUTPARAMETERS OF THE SYSTEM
CSUCH AS TORQUE,SPEED,VARF

```

SUBROUTINE OUTP(X,Y,DERY,IHLF,NDIM,PRMT)
REAL L,INVL,IS
INTEGER P,NA
COMMON /MIT/L,R,P,RJ,RK,V,INVL,DERL,NA,TIME,TORQUE,VARF,SPEED,
XIS,PDERL,NR
DIMENSION Y(10),DERY(10),CUR(6),PDERL(6,6),TI(1,6),PDERLI(6),
XTORQUE(705),SPEED(705),VARF(705),L(6,6),R(6,6),V(8),
XINVL(6,6),DERL(6,6),TIME(705),IS(705),PRMT(5)
PIA=22./7.
DO 1 K=1,6
  CUR(K)=Y(K)
1 CONTINUE
  N=6
  K=1
  CALL MATPLY(PDERLI,PDERL,CUR,N,N,K)
  DO 2 J=1,6
    TI(1,J)=CUR(J)
  2 N=1
  M=6
  K=1
  CALL MATPLY(TDERLI,TI,PDERLI,N,M,K)
  NA=NA+1
  TIME(NA)=X
  IS(NA)=Y(1)
  TORQUE(NA)=TDERLI*.001.
  OMGM=Y(7).
  SPEED(NA)=OMGM*60./(2.*PIA)

```

C OPTICAL ENCODER OUTPUT FOR THE DISC OF 36 HOLES MOUNTED ON THE SHAFT

```

  VARF(NA)=OMGM*36/(2.*PIA)
  C WRITE (6,6) V(1),V(2),V(3),Y(7),Y(9),Y(10),DERY(10)
  6 FORMAT ('0',7(E15.7,2X))
  5 CONTINUE
  RETURN
  END

```

Cont.

CTHIS SUBROUTINE DO THE INVERSION OF MATRIX A(N,N) BY USING AUXILIARY
C MATRIX H(N,2*N) AND AUGUMENTING THE MATRIX A WITH THE UNIT MATRIX OF
C SAME DIMENSION (N,N)

```
SUBROUTINE MATINV(INVA,A,N,N2,H)
REAL INVA
DIMENSION A(6,6),INVA(6,6),H(6,12)
DO 1 I=1,N
DO 1 J=1,N
1 H(I,J)=A(I,J)
N1=N+1
DO 2 I=1,N
DO 3 J=N1,N2
N3=I+N
IF (N3-J) 4,5,4
5 H(I,J)=1.0
GO TO 3
4 H(I,J)=0.0
3 CONTINUE
2 CONTINUE
DO 6 I=1,N
D=H(I,I)
DO 7 J=1,N2
7 H(I,J)=H(I,J)/D
DO 8 L=1,N
IF (L.EQ.I) GO TO 8
E=H(L,I)
DO 9 J=1,N2
9 H(L,J)=H(L,J)-E*H(I,J)
8 CONTINUE
6 CONTINUE
DO 10 I=1,N
DO 10 J=N1,N2
10 INVA(I,J-N)=H(I,J)
RETURN
END
```

C
C
C THIS SUBROUTINE MATPLY DO THE MULTIPLICATION OF TWO MATRIX
C A(N,M) AND B(M,L)
C

```
SUBROUTINE MATPLY(AB,A,B,N,M,L)
DIMENSION AB(N,L),A(N,M),B(M,L)
DO 1 K=1,N
DO 2 I=1,L
SUM=0.0
DO 3 J=1,M
SUM=SUM+A(K,J)*B(J,I)
3 CONTINUE
AB(K,I)=SUM
2 CONTINUE
1 CONTINUE
RETURN
END
```

Program No.3 - System without harmonics simulated, avoiding matrix inversion in every step of integration

THIS PROGRAM WILL DO DIGITAL SIMULATION OF TIME DOMAIN SPACE MODEL FOR INDUCTION MOTOR SPEED CONTROL USING PHASE LOCKED LOOP TECHNIQUE, IT ALSO PLOTS SPEED, TORQUE, CURRENT, ACCELERATION CHARACTERISTICS

INDUCTION MOTOR USED. - 30HP, 220V, 60HZ, 4-POLE, STAR CONNECTED
TORQUE EQUATION TE=TL+0.06WM+0.03WM

BLOCK DATA TO READ COMMON PARAMETERS IN MAIN PROGRAM & SUBROUTINES OF THIS SYSTEM

BLOCK DATA

REAL LSR, K1, K2, K3, K4, K5

INTEGER P

COMMON/PARA/ SR(3,3), RR(3,3), SSL(3,3), P, LSR, AJ, AK, PIA, TL, K1, K2, K3, K4, K5, VM, WC

COMMON/FUN/ SSLI(3,3), V(3), SRL(3,3), RSL(3,3), DSRL(3,3), SI(3), RI(3), SRI(3), DSRLI(3), SUMS(3), SMUL1(3), SMUL2(3), RRI(3), DRSLI(3), SUMR(3), SMULR(3), CI(6), PDL(6,6), TI(1,6), PDLI(6), TERM, DRSL(3,3), DSI(3), DRI(3), SRLDRI(3), RSLDSI(3)

COMMON/OUT/NA, TIME(1205), SPEED(1205), CUR(1205), TORQUE(1205), ACCEL(1205)

DATA SR, RR, SSL, P, LSR, AJ, AK/0.063, 3*0.0, 0.063, 3*0.0, 0.063, 0.083, 3*0.0, 0.083, 3*0.0, 0.083, 0.0203925, 3*-0.01, 0.0203925, 3*-0.01, 0.0203925, 4, 0.02, 0.06, 0.03/

DATA TL, K1, K2, K3, K4, K5, VM, WC/0.0, 0.0021167, 198.4164, 0.19, 2.28, 9.12, 160.0, 2261.9467/

DATA NA, PIA/0, 3.142857/

END

NOW MAIN PROGRAM OF THE SYSTEM USING RKGS FOR SOLVING A SET OF NON-LINEAR DIFFERENTIAL EQUATIONS:

REAL LSR, K1, K2, K3, K4, K5

INTEGER P

COMMON/PARA/ SR(3,3), RR(3,3), SSL(3,3), P, LSR, AJ, AK, PIA, TL, K1, K2, K3, K4, K5, VM, WC

Cont.

X
X
X
X
C
X
C
1
C
C
C
2
3
X
5
4
C
C
C
C
C
C
C
C
C
C
X
C

```
COMMON/FUN/SSLI(3,3),V(3),SRL(3,3),RSL(3,3),DSRL(3,3),  
SI(3),RI(3),SRI(3),DSRLI(3),SUMS(3),SMUL1(3),  
SMUL2(3),RRI(3),DRSLI(3),SUMR(3),SMULR(3),  
CI(6),PDL(6,6),TI(1,6),PDLI(6),TERM,DRSL(3,3),  
DSI(3),DRI(3),SRLDRI(3),RSLDSI(3)
```

```
COMMON/OUT/NA,TIME(1205),SPEED(1205),CUR(1205),  
TORQUE(1205),ACCEL(1205)
```

```
DIMENSION Y(11),DERY(11),PRMT(5),AUX(4,11)  
EXTERNAL CRKS,FCT,OUTP,MATINV,MATPLY  
DO 1 I=1,11  
Y(I)=0.0  
DERY(I)=1./11.
```

```
CONTINUE  
Y(9)=2.5  
Y(10)=5.7  
NDIM=11  
PRMT(1)=0.0  
PRMT(2)=0.36  
PRMT(3)=0.0003  
PRMT(4)=0.00001  
PRMT(5)=0.0
```

```
CALL CRKS (PRMT,Y,DERY,NDIM,IHLF,FCT,OUTP,AUX)
```

```
WRITE THE STATOR CURRENT,SPEED,TORQUE,TIME
```

```
WRITE (6,2) NA  
FORMAT(2X,I5//)  
WRITE (6,3)  
FORMAT('0',2X,'TIME',T24,'STATOR CURRENT',T44,'TORQUE',  
T62,'SPEED'//)  
DO 4 I=1,NA  
WRITE (6,5) TIME(I),CUR(I),TORQUE(I),SPEED(I)  
FORMAT('0',4(E15.7,10X))  
CONTINUE
```

THIS PROGRAM PLOTS THE STATOR CURRENT VS TIME

```
SELECT SIZE OF PAPER,30CM X 27.5CM  
CALL PLOTS (30.0,27.5)
```

```
SET THE ORIGIN  
CALL PLOT (2.5,2.5,-3)
```

```
CALL SCALE (TIME,25.0,1201,1)  
CALL SCALE (SPEED,20.0,1201,1)
```

```
TITLE THE X-AXIS AND DO SCALING  
CALL AXIS (0.0,0.0,10HTIME (SEC),-10,25.0,0.0,  
TIME(1202),TIME(1203))
```

Cont.

C TITLE THE Y-AXIS AND DO SCALING
CALL AXIS (0.0,0.0,14HSPEED (R.P.M.),14,20.0,90.0,
X SPEED(1202),SPEED.(1203))

C PLOT IS VS TIME IN BLACK INK
CALL LINE (TIME,SPEED,1201,1,0.0)

C WRITE TITLE OF THE PLOT
CALL SYMBOL (5.0,20.0,0.35,22H SPEED VS TIME,
X 0.0,22)

C STOP PLOTTING
CALL PLOT (0.0,0.0,999)

C STOP
END

C RUNGE KUTTA GILL CLASSICAL SUBROUTINE
SUBROUTINE CRKS(PRMT,Y,DERY,NDIM,IHLF,FCT,OUTP,AUX)
C DIMENSION Y(11),DERY(11),PRMT(5),AUX(4,11),YY(11)
X=PRMT(1)
XEND=PRMT(2)
H=PRMT(3)
IHLF=0

1 IF(X-XEND) 2,2,9
2 CALL FCT(X,Y,DERY)
CALL OUTP(X,Y,DERY,IHLF,NDIM,PRMT)
DO 7 K=1,4
DO 6 I=1,NDIM
GO TO (3,4,4,5),K
3 YY(I)=Y(I)
GO TO 6
4 YY(I)=Y(I)+AUX(K-1,I)*0.5
GO TO 6
5 YY(I)=Y(I)+AUX(K-1,I)
6 CONTINUE
CALL FCT(X,YY,DERY)
DO 7 I=1,NDIM
AUX(K,I)=H*DERY(I)
DO 8 I=1,NDIM
DY=(AUX(1,I)+2.0*AUX(2,I)+2.0*AUX(3,I)+AUX(4,I))/6.0
8 Y(I)=Y(I)+DY
X=X+H
GO TO 1
9 RETURN
END

C THIS FUNCTION SUBROUTINE DEVELOP THE SYSTEM EQUATION IN TIME
C DOMAIN

C SUBROUTINE FCT (X,Y,DERY)

C REAL LSR,K1,K2,K3,K4,K5

C INTEGER P

C COMMON/PARA/ SR(3,3),RR(3,3),SSL(3,3),P,LSR,AJ,AK,PIA,
X TL,K1,K2,K3,K4,K5,VM,WC

```

COMMON/FUN/SSLI(3,3),V(3),SRL(3,3),RSL(3,3),DSRL(3,3),
SI(3),RI(3),SRI(3),DSRLI(3),SUMS(3),SMUL1(3),
SMUL2(3),RRI(3),DRSLI(3),SUMR(3),SMULR(3),
CI(6),PDL(6,6),TI(1,6),PDLI(6),TERM,DRSL(3,3),
DSI(3),DRI(3),SRLDRI(3),RSLDSI(3)

COMMON/OUT/NA,TIME(1205),SPEED(1205),CUR(1205),
TORQUE(1205),ACCEL(1205)

DIMENSION Y(11),DERY(11),H(3,6)
DEVELOPMENT OF CONTROL VECTOR V

PHASE CONTROLLED RECTIFIER OUTPUT VCO
ALPHA=K3*Y(10)
IF (DERY(11).GT.377) ALPHA=0.0
VCO=3.*SQRT(2.)*VM*COS(ALPHA)/PIA

SIX STEP INVERTER OUTPUT V(I) ONLY FUNDAMENTAL
V(1)=3.*VCO*SIN(Y(11))/PIA
V(2)=3.*VCO*SIN(Y(11)-2.*PIA/3.)/PIA
V(3)=3.*VCO*SIN(Y(11)+2.*PIA/3.)/PIA

CALCULATE INVERSION OF SELF INDUCTANCE MATRIX SSL=RRL IF X=0.0
IF (X.GT.0.0) GO TO 1
K=3
M=6
CALL MATINV (SSLI,SSL,K,M,H)

CONTINUE
EVALUATE TIME DEPENDENT TERMS:
DEVELOP MUTUAL INDUCTANCE MATRIX SRL

SRL(1,1)=LSR*COS(Y(8))
SRL(1,2)=LSR*COS(Y(8)+2.*PIA/3.)
SRL(1,3)=LSR*COS(Y(8)-2.*PIA/3.)
SRL(2,1)=SRL(1,3)
SRL(2,2)=SRL(1,1)
SRL(2,3)=SRL(1,2)
SRL(3,1)=SRL(1,2)
SRL(3,2)=SRL(1,3)
SRL(3,3)=SRL(1,1)

DEVELOP MUTUAL INDUCTANCE MATRIX RSL=(SRL)
DO 2 I=1,3
DO 2 J=1,3
RSL(I,J)=SRL(J,I)

CONTINUE

CALCULATE TIME DERIVATIVE OF SRL & RSL
DSRL(1,1)=-LSR*SIN(Y(8))*DERY(8)
DSRL(1,2)=-LSR*SIN(Y(8)+2.*PIA/3.)*DERY(8)
DSRL(1,3)=-LSR*SIN(Y(8)-2.*PIA/3.)*DERY(8)
DSRL(2,1)=DSRL(1,3)
DSRL(2,2)=DSRL(1,1)
DSRL(2,3)=DSRL(1,2)
DSRL(3,1)=DSRL(1,2)
DSRL(3,2)=DSRL(1,3)
DSRL(3,3)=DSRL(1,1)

```

Cont.

C
C
3
C
C
4
C
C
C
5
C
C
C
6
C
C
C
7
C
C
8

```
DO 3 I=1,3  
DO 3 J=1,3  
  DSRL(I,J)=DSRL(J,I)  
CONTINUE
```

```
CALCULATE STATOR CURRENT & ROTOR MATRIX  
DO 4 I=1,3  
  SI(I)=Y(I)  
  RI(I)=Y(I+3)  
  DRI(I)=DERY(I+3)  
CONTINUE
```

```
DEVELOPMENT OF STATOR VOLTAGE EQUATIONS  
MULTIPLICATION OF SR TO SI  
  K=3  
  M=1  
  CALL MATPLY (SRI,SR,SI,K,K,M)  
MULTIPLICATION OF DSRL TO RI  
  CALL MATPLY (DSRLI,DSRL,RI,K,K,M)  
MULTIPLICATION OF SRL TO DRI  
  CALL MATPLY (SRLDRI,SRL,DRI,K,K,M)  
SUM OF SRI , DSRLI & SRLDRI  
DO 5 I=1,3  
  SUMS(I)=SRI(I)+DSRLI(I)+SRLDRI(I)  
CONTINUE  
MULTIPLICATION OF SUMS TO SSLI  
  CALL MATPLY (SMUL1,SSLI,SUMS,K,K,M)  
MULTIPLICATION OF V TO SSLI  
  CALL MATPLY (SMUL2,SSLI,V,K,K,M)  
DO 6 I=1,3  
  DERY(I)=-SMUL1(I)+SMUL2(I)  
  DSI(I)=DERY(I)  
CONTINUE
```

```
DEVELOPMENT OF ROTOR VOLTAGE EQUATIONS  
MULTIPLICATION OF RR TO RI  
  K=3  
  M=1  
  CALL MATPLY (RRI,RR,RI,K,K,M)  
MULTIPLICATION OF DRSL TO SI  
  CALL MATPLY (DRSLI,DRSL,SI,K,K,M)  
MULTIPLICATION OF RSL TO DSI  
  CALL MATPLY (RSLDSI,RSL,DSI,K,K,M)  
SUM OF RRI , DRSLI & RSLDSI  
DO 7 I=1,3  
  SUMR(I)=RRI(I)+DRSLI(I)+RSLDSI(I)  
CONTINUE  
MULTIPLICATION OF SUMR TO SSLI  
  CALL MATPLY (SMULR,SSLI,SUMR,K,K,M)  
DO 8 I=1,3  
  DERY(I+3)=-SMULR(I)  
CONTINUE
```

Cont.

DEVELOPMENT OF TORQUE & SPEED EQUATIONS

DO 9 I=1,3

CI(I)=Y(I)

CI(I+3)=Y(I+3)

CONTINUE

FIND TRANSPOSE OF CI

DO 10 I=1,6

TI(1,I)=CI(I)

CONTINUE

DEVELOP PARTIAL DERIVATIVE OF INDUCTANCE MATRIX

PDL(1,4)=-LSR*SIN(Y(8))

PDL(1,5)=-LSR*SIN(Y(8)+2.*PIA/3.)

PDL(1,6)=-LSR*SIN(Y(8)-2.*PIA/3.)

PDL(2,4)=PDL(1,6)

PDL(2,5)=PDL(1,4)

PDL(2,6)=PDL(1,5)

PDL(3,4)=PDL(1,5)

PDL(3,5)=PDL(1,6)

PDL(3,6)=PDL(1,4)

DO 11 I=1,3

DO 11 J=1,3

PDL(I,J)=0.0

PDL(J+3,I)=PDL(I,J+3)

PDL(I+3,J+3)=0.0

CONTINUE

MULTIPLICATION OF PDL TO CI

K=6

M=1

CALL MATPLY(PDLI,PDL,CI,K,K,M)

MULTIPLICATION OF TI TO PDLI

K=1

M=6

N=1

CALL MATPLY(SPDLI,TI,PDLI,K,M,N)

TERM=SPDLI*P/(AJ*4)

DERY(7)=TERM-AK*Y(7)/AJ-TL/AJ

DERY(8)=P*Y(7)/2.

DEVELOPMENT OF EQUATIONS FOR ELECTRONIC PART OF THE SYSTEM

PHASE DETECTOR ERROR VOLTAGE (VE)

DERY(9)=-2.*PIA*K1*DERY(7)

FILTER OUTPUT

DERY(10)=K4*DERY(9)+K5*Y(9)

VCO FREQUENCY & INVERTER FREQUENCY

DERY(11)=(WC-K2*Y(10))/6.

RETURN

END

Cont.....

THIS OUTP-SUBROUTINE WILL BE USED TO STORE & PRINT THE DATA

SUBROUTINE OUTP(X,Y,DERY,IHLF,NDIM,PRMT)

REAL LSR,K1,K2,K3,K4,K5
INTEGER P
COMMON/PARA/ SR(3,3),RR(3,3),SSL(3,3),P,LSR,AJ,AK,PIA,
TL,K1,K2,K3,K4,K5,VM,WC

COMMON/FUN/SSLI(3,3),V(3),SRL(3,3),RSL(3,3),DSRL(3,3),
SI(3),RI(3),SRI(3),DSRLI(3),SUMS(3),SMUL1(3),
SMUL2(3),RRI(3),DBSLI(3),SUMR(3),SMULR(3),
CI(6),PDL(6,6),TI(1,6),PDLI(6),TERM,DRSL(3,3),
DSI(3),DRI(3),SRLDRI(3),RSLDSI(3)

COMMON/OUT/NA,TIME(1205),SPEED(1205),CUR(1205),
TORQUE(1205),ACCEL(1205)

DIMENSION Y(11),DERY(11),PRMT(5)

STORE THE DATA FOR PLOTTING & PRINTING

NA=NA+1
TIME(NA)=X
SPEED(NA)=Y(7)*60./(2.*PIA)
CUR(NA)=Y(1)
TORQUE(NA)=TERM*AJ
ACCEL(NA)=DERY(7)

WRITE (6,6) X,Y(7),Y(8),Y(9),Y(10),Y(11),DERY(11)
FORMAT ('0',7(E15.7,2X))
RETURN
END

THIS SUBROUTINE DO THE INVERSION OF MATRIX A(N,N) BY USING AUXILIARY
MATRIX H(N,2*N) AND AUGMENTING THE MATRIX A WITH THE UNIT MATRIX OF
SAME DIMENSION (N,N)

SUBROUTINE MATINV(INVA,A,N,N2,H)
REAL INVA
DIMENSION A(3,3),INVA(3,3),H(3,6)
DO 1 I=1,N
DO 1 J=1,N
1 H(I,J)=A(I,J)
N1=N+1
DO 2 I=1,N
DO 3 J=N1,N2
N3=I+N
IF (N3-J) 4,5,4
5 H(I,J)=1.0

Cont.

```

4 GO TO 3
3 H(I,J)=0.0
2 CONTINUE
CONTINUE
DO 6 I=1,N
D=H(I,I)
DO 7 J=1,N2
7 H(I,J)=H(I,J)/D
DO 8 L=1,N
IF (L.EQ.I) GO TO 8
E=H(L,I)
DO 9 J=1,N2
9 H(L,J)=H(L,J)-E*H(I,J)
8 CONTINUE
6 CONTINUE
DO 10 I=1,N
DO 10 J=N1,N2
10 INVA(I,J-N)=H(I,J)
RETURN
END

```

C
C
C
C
C
C

C THIS SUBROUTINE MATPLY DO THE MULTIPLICATION OF TWO MATRIX
C A(N,M) AND B(M,L)

```

SUBROUTINE MATPLY(AB,A,B,N,M,L)
DIMENSION AB(N,L),A(N,M),B(M,L)
DO 1 K=1,N
DO 2 I=1,L
SUM=0.0
DO 3 J=1,M
SUM=SUM+A(K,J)*B(J,I)
3 CONTINUE
AB(K,I)=SUM
2 CONTINUE
1 CONTINUE
RETURN
END

```

REFERENCES

1. R. Moffat, P. Sen, R. Younker & M. M. Boyoni, "Digital Phase Locked Loop for Induction Motor Speed Control", IEEE Trans. on Industrial Applications, Vol. IA-15, No. 2, March/April 1979.
2. Hoang Le-Huy, "A Synchronous Thyristorised D.C. Motor Drive", IEEE Trans. on Industrial Applications, Vol. IA-15, No. 2, March/April 1979.
3. Jacob Tal, "Speed Control By Phase Locked Servo Systems- New Possibilities and Limitations", IEEE Trans. on Industrial Electronics & Control Instrumentation, Vol. IECI-24, No. 1, February 1977.
4. A. W. Moore, "Phase Locked-Loops for Motor Speed Control", IEEE Spectrum, April 1973.
5. S. A. Nasar and J. B. Scott, "Time Domain Formulation of The Dynamics of Induction Motors", Int. J. Elect. Engg. Educ., Vol. 11, pp 36-44, Manchester, U.K., 1973.
6. P. J. Lawrenson and J. M. Stephenson, "Note on Induction Machine Performance with a Variable Frequency Supply", Proc. IEE, Vol. 113, No. 10, October 1966.
7. I. R. Smith and S. Sriharan, "Transient Performance of The Induction Motor", Proc. IEE, Vol. 113, No. 7, July 1966.
8. M. L. MacDonald and P. Sen, "Control Loop Study of Induction Motor Drives Using D-Q Model", IEEE Trans. on Industrial Electronics & Control Instrumentation, Vol. IECI-26, No. 4, Nov. 1979.
9. S. B. Dewan and A. Straughen, "Power Semiconductor Circuits", John Wiley & Sons, Inc., New York, 1975.
10. M. Mittal and N. U. Ahmed, "Time Domain Modelling And Digital Simulation of Variable Frequency A.C. Motor Speed Control using PLL Technique", IEEE's 1981 Industrial Applications Society Annual Meeting, Philadelphia, PA, Oct. 5-9, 1981.
11. J. M. D. Murphy, "Thyristor Control of A.C. Motors", Pergamon Press, New York, 1973.

12. R.S. Ramshaw, "Power Electronics-Thyristor Controlled Power for Electric Motors", Chapman And Hall, London, 1973.
13. -----, "SCR Manual - including Triacs & other Thyristors", Sixth Edition, General Electric Company, New York, 1979.
14. John D. Link, "Logic Designer's Manual", Prentice-Hall, Virginia, 1977.
15. Bimal K. Bose, "Adjustable Speed AC Drive Systems", IEEE Press, N.J., 1981.
16. Floyd M. Gardner, "Phase-Lock Techniques", Second Edition, John Wiley & Sons, Inc., New York, 1979.